Dissertation

The role of phosphoenolpyruvate carboxykinase in lung cancer

submitted by

Dr. med. univ. Katharina LEITHNER

for the Academic Degree of

Doctor of Philosophy (PhD)

at the

Medical University of Graz

Division of Pulmonology

Department of Internal Medicine

Austria

under the Supervision of

Univ. Prof. Dr. Horst Olschewski

2014

Statutory Declaration

I hereby declare that this dissertation is my own original work and that I have fully acknowledged by name all of those individuals and organizations that have contributed to the research for this dissertation. Due acknowledgement has been made in the text to all other material used. Throughout this dissertation and in all related publications I followed the guidelines of “Good Scientific Practice”. The major part of this thesis has been published in (Leithner et al., 2014b).

Graz, January 14, 2014 *Katharina Leithner*

Acknowledgements

I would like to thank my supervisor Prof. Dr. Horst Olschewski for his constant support and for his enthusiasm to follow up new ideas. I am grateful for the valuable advice and help with planning of experiments, daily lab-work and with scientific writing by our group leader, co-supervisor and thesis committee member Assoc. Prof. Dr. Andelko Hrzenjak, Division of Pulmonology, Medical University of Graz. I would like to thank the thesis committee member Prof. DDr. Andrea Olschewski, Director of the Ludwig Boltzmann Institute for Lung Vascular Research, Graz, for her excellent mentorship and for giving our lung cancer group the opportunity to work in close collaboration with her Institute. I thank the thesis committee member Prof. Dr. Berthold Huppertz, Institute of Cell Biology, Histology and Embryology, Medical University of Graz, for his support and advice. I am grateful to Prof. Dr. Gerald Höfler, Institute of Pathology, Medical University of Graz, for evaluating the thesis together with Prof. Dr. Horst Olschewski. I would further like to thank Dr. Christoph Wohlkönig PhD, for his constant help with human material and patient data and Alexandra Bertsch and Elisabeth Pöllitzer, Division of Pulmonology, Medical University of Graz, for their excellent technical assistance.

The excellent cooperation with Dr. Elvira Stacher-Priehse, Institute of Pathology, Medical University of Graz, is highly appreciated. I thank Dr. Harald Köfeler, Dr. Martin Trötzmüller, and Astrid Knopf, Core Facility Mass Spectrometry at the Center for Medical Research (CMR, ZMF), Medical University of Graz, for performing mass-spectrometry analyses and for helpful discussions. I am grateful to Prof. Dr. Rudolf Zechner, Institute of Molecular Biosciences, Karl Franzens University, Graz, for his advice and valuable discussions. I am indebted to Prof. Dr. Adrian L. Harris, Weatherall Institute of Molecular Medicine, University of Oxford, Oxford, United Kingdom, for giving me the opportunity to discuss my projects in his lab and to get to know the spheroid model developed in his Institute, for valuable discussions and for critical reading of the manuscript. The contribution by Dr. Tarek Moustafa, Institute of Molecular Biosciences, Karl Franzens University, Graz, and Dr. Jörg Lindenmann, Division of Thoracic and Hyperbaric

Surgery, Department of Surgery, Medical University of Graz, to the present study is highly appreciated. I would also like to thank all co-authors of the project on lung cancer hypoxia (Leithner et al., 2014a; see also 10.2.), which I conducted in parallel. Finally, I thank my family, Andreas, Miriam, Arthur, and Georg for their patience and support.

Table of Contents

1. Abbreviations

3-MP	3-mercaptopicolinate
ALK	anaplastic lymphoma kinase
AMPK	AMP-activated protein kinase
BSA	bovine serum albumin
CREB	cAMP response element binding
CRTC2	CREB regulated transcriptional coactivator 2
EML	echinoderm microtubule-associated protein-like 4
ER	endoplasmic reticulum
FA	fatty acid
FBP	fructose-1,6-biphosphatase
FBS	fetal bovine serum
FDG-PET	^{18}F-desoxyglucose positron emission tomography
GEO	Gene Expression Omnibus
HDAC	histone deacetylase
HNF4α	hepatocyte nuclear factor 4α
IHC	immunohistochemistry
KRAS	Kristen rat sarcoma viral oncogene
LC-MS	liquid chromatography – mass spectrometry
LKB1	liver kinase B1
MCT1	monocarboxylate transporter 1
MCT4	monocarboxylate transporter 4
NADH	reduced nicotinamide adenine dinucleotide
NADPH	reduced nicotinamide adenine dinucleotide phosphate
NSCLC	non-small cell lung cancer
PCK1	cytoplasmic isoform of phosphoenolpyruvate carboxykinase
PCK2	mitochondrial isoform of phosphoenolpyruvate carboxykinase
PEP	phosphoenolpyruvate
PEPCK	phosphoenolpyruvate carboxykinase
PGC-1α	peroxisome proliferator–activated receptor γ coactivator 1
PI	propidium iodide
PKM2	M2 isoform of pyruvate kinase
PPP	pentose phosphate pathway
qPCR	quantitative real-time PCR
shRNA	short hairpin RNA
siRNA	small interfering RNA
STK11	serine-threonine kinase 11
TCA cycle	tricarboxylic acid cycle
VEGF	vascular endothelial growth factor

2. Abstract (German)

In soliden Tumoren wie dem Bronchialkarzinom sind Areale mit Sauerstoff- und Nährstoffmangel, insbesonders Glucosemangel, häufig. Die Mechanismen der Anpassung der Tumorzellen an den chronischen Mangel an Glucose sind bisher kaum bekannt. Gluconeogenese, die Neubildung von Glucose aus kleinen Molekülen, ist ein Stoffwechselweg, der vor allem in normalen Leberzellen aktiv ist. Das Schlüsselenzym der Gluconeogenese ist die Phosphoenolpyruvat Carboxykinase (PEPCK). Obwohl die PEPCK potentiell wichtige Bestandteile für die Zellteilung und das Zellwachstum liefern kann, ist ihre Rolle für das Tumorwachstum völlig ungeklärt.

In dieser Studie konnten wir zeigen, dass PEPCK Aktivität in Lungenkrebszelllinien vorhanden ist, und dass die Expression der mitochondrialen Form des Enzyms (PCK2) sowie die PEPCK Aktivität unter Glucosemangel zunehmen. Weiters konnten wir zeigen, dass in Lungenkrebsproben operierter Patienten die PEPCK-Aktivität im Vergleich zu normaler Lunge signifikant erhöht ist. Um definitiv diesen neuen metabolischen Pathway in Lungenkrebszellen nachzuweisen, wurde stabil isotopmarkiertes Laktat ($^{13}C_3$-Laktat) angewandt und die Konversion zu $^{13}C_3$-Phosphoenolpyruvat bestimmt. Unter Wachstumsbedingungen mit niedriger Glucose- und hoher Laktatkonzentration, wie sie typischerweise in soliden Tumoren zu finden sind, kam es zu einer Anreicherung von $^{13}C_3$-Phosphoenolpyruvat. Damit gelang der Nachweis des Stoffwechselweges von Laktat zu Phosphoenolpyruvat über Pyruvat Carboxylase und PEPCK. Die Hemmung der PCK2 mittels 3-Mercaptopicolinat und siRNA führte zu einer signifikanten Zunahme der Glucosemangel-bedingten Apoptose in Lungenkrebszellen mit einer Mutation des Energiesensors LKB1 (lymphoma kinase B1). Weiters führte 3-Mercaptopicolinat zu einer Reduktion des Wachstums von Krebszell-Spheroiden. Die Studie liefert damit erstmals den Nachweis, dass zumindest bestimmte Abschnitte der Gluconeogenese ausgehend von Laktat in Lungenkrebszellen aktiv sind, und dass dies das Überleben der Zellen unter Glucosemangel begünstigt.

3. Abstract (English)

Cancer cells are re-programmed to utilize glycolysis at high rates, which provides building blocks for cell growth. Consequently, glucose levels may decrease substantially in underperfused tumor areas. Gluconeogenesis, the generation of glucose from small carbon substrates, is the reverse of glycolysis in many aspects, but differs in the requirement for phosphoenolpyruvate carboxykinase (PEPCK) and fructose-1,6-biphosphatase. PEPCK, which generates phosphenolpyruvate (PEP) from oxaloacetate, has been shown to provide metabolites for cell growth. Still, the role of PEPCK in cancer is unknown. In the present work it is shown that the mitochondrial isoform of PEPCK (PCK2) is expressed and active in lung cancer cell lines and in non-small cell lung cancer samples. PCK2 expression and activity were enhanced under low glucose. PEPCK activity was elevated threefold in lung cancer samples over normal lungs and contributed to the PEP pool under low glucose, as shown by stable isotope analyses using $^{13}C_3$-lactate. PEPCK inhibition using 3-mercaptopicolinate or PCK2 siRNA significantly enhanced glucose depletion-induced apoptosis in lung cancer cells carrying an inactivating LKB1 (lymphoma kinase B1) mutation. Furthermore, 3-mercaptopicolinate significantly reduced the growth of multicellular spheroids. In conclusion, lung cancer cells utilize at least some steps of gluconeogenesis and by this way adapt to glucose deprivation.

4. Introduction

4.1. Lung cancer

Lung cancer accounts for most cancer deaths worldwide (Ramalingam et al., 2011). Approximately 85% of lung cancers are non-small cell lung cancers (NSCLC) and 15% are small-cell lung cancers. NSCLCs are often advanced at diagnosis (Ramalingam et al., 2011). Despite treatment the overall survival remains poor, mainly due to late diagnosis (Roberts et al., 2010). The overall five-year survival is between 6% and 14% in men, and between 7% and 18% in women (Cagle, 2010). In stage I, II or IIIA (IIIB) surgery is attempted with curative intent, eventually in combination with adjuvant chemotherapy. In advanced disease (stage IIIB, regionally advanced with lymph node metastases and stage IV with distant metastases) platinum-based chemotherapy is the backbone of treatment and provides a survival benefit when compared with best supportive care (Reck et al., 2013; Socinski, 2004). For a limited proportion of patients with specific activating mutations of the epidermal-growth factor receptor or chromosomal rearrangements leading to echinoderm microtubule-associated protein-like 4 (EML) - anaplastic lymphoma kinase (ALK) fusion proteins, targeted therapies are available as first - line therapies. Although initial response rates are high with these treatments, recurrences are frequent (Reck et al., 2013). However, in the majority of lung cancer patients such targetable genetic alterations are absent. Thus, research on novel cellular signaling and metabolic pathways is a current promise.

4.2. Role of the microenvironment in cancer growth

Solid cancers, like lung cancer, are dependent on the growth of new blood vessels (angiogenesis) as soon as the tumors become larger than 1 mm^3 (Vaupel, 2008). Due to the irregular and aberrant growth pattern of the newly formed blood vessels and due to rapid tumor growth, the supply with oxygen and nutrients is often inadequate (Vaupel, 2008). The resulting lack of oxygen (hypoxia) is known to play a central role in cancer progression and therapy resistance (Vaupel, 2008). As we

could show recently, hypoxia-induced resistance in lung cancer cells towards the platinum drug cisplatin is associated with stabilization of hypoxia-inducible factor 1α (HIF-1α) and down-regulation of the apoptosis protein B-cell lymphoma 2-associated X protein (BAX) (Wohlkoenig et al., 2011). Importantly we found that adaptation to hypoxia and hypoxia-induced apoptosis resistance were reversible (Wohlkoenig et al., 2011).

Similar to oxygen, glucose levels decrease in underperfused tumor areas (Cantor and Sabatini, 2012) (Figure 1). In fact the glucose concentration has been shown to be highly variable in solid cancers (Schroeder et al., 2005; Walenta et al., 2001). Recent studies confirmed that glucose levels are lower in tumors compared to corresponding normal tissues (Hirayama et al., 2009; Rocha et al., 2010). However the mechanisms of adaptation of cancer cells to glucose depletion and its role in cancer progression are poorly understood.

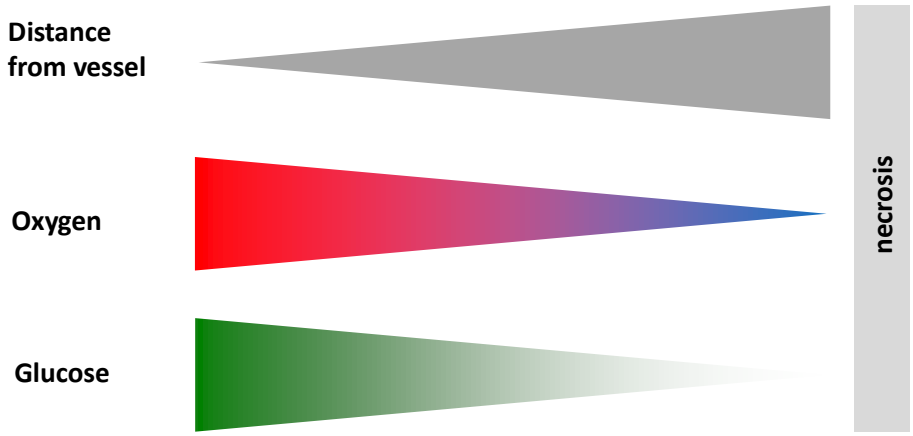

Figure 1. Gradients for oxygen and glucose in the microenvironment of solid cancers.

4.3. Glucose metabolism in cancer cells

Rapidly growing cancers, including lung cancer, utilize large amounts of glucose (Cairns et al., 2011; DeBerardinis and Thompson, 2012; Schulze and Harris, 2012; Vander Heiden et al., 2009). The high uptake of glucose by tumor cells is the

underlying mechanism in ^{18}F-desoxyglucose positron emission tomography (FDG-PET), a routinely used diagnostic imaging technique in the clinical staging of cancer patients (Bensinger and Christofk, 2012).

In cancer cells glucose is metabolized primarily by glycolysis, while the tricarboxylic cycle (TCA cycle, Krebs cycle) is largely bypassed, although still active (Cairns et al., 2011; DeBerardinis and Thompson, 2012; Schulze and Harris, 2012; Vander Heiden et al., 2009). This “aerobic glycolysis” has been described by the Nobel laureate Otto Heinrich Warburg as early as 1924 and is called the „Warburg effect“ (Koppenol et al., 2011). The Warburg effect, which is observed in cancer cells but also other highly proliferative cells, ensures the generation of building blocks for cell growth. It enhances flux of glycolytic metabolites through to the oxidative and non-oxidative branches of the pentose phosphate pathway (PPP), thus providing NADPH (reduced nicotinamide adenine dinucleotide phosphate) and ribose (Cairns et al., 2011; DeBerardinis and Thompson, 2012; Schulze and Harris, 2012; Vander Heiden et al., 2009) (Figure 2). Furthermore glucose may be diverted to glycerol and serine synthesis (Kalhan and Hanson, 2012) (Figure 2). The mechanisms underlying the Warburg effect have been extensively studied in the past years. Expression of the embryonic M2 form of pyruvate kinase (PKM2), which is the isoform largely expressed in tumor cells, plays a central role (Christofk et al., 2008).

Otto Warburg himself stated that “fermentation [glycolysis] decreases in the direction of capillary blood-flow” in cancers in vivo, based on the observed low glucose concentration in rat tumor veins (Warburg et al., 1927). Given the importance of (aerobic) glycolysis in tumor growth the question arises, how tumor cells adapt to conditions of glucose depletion.

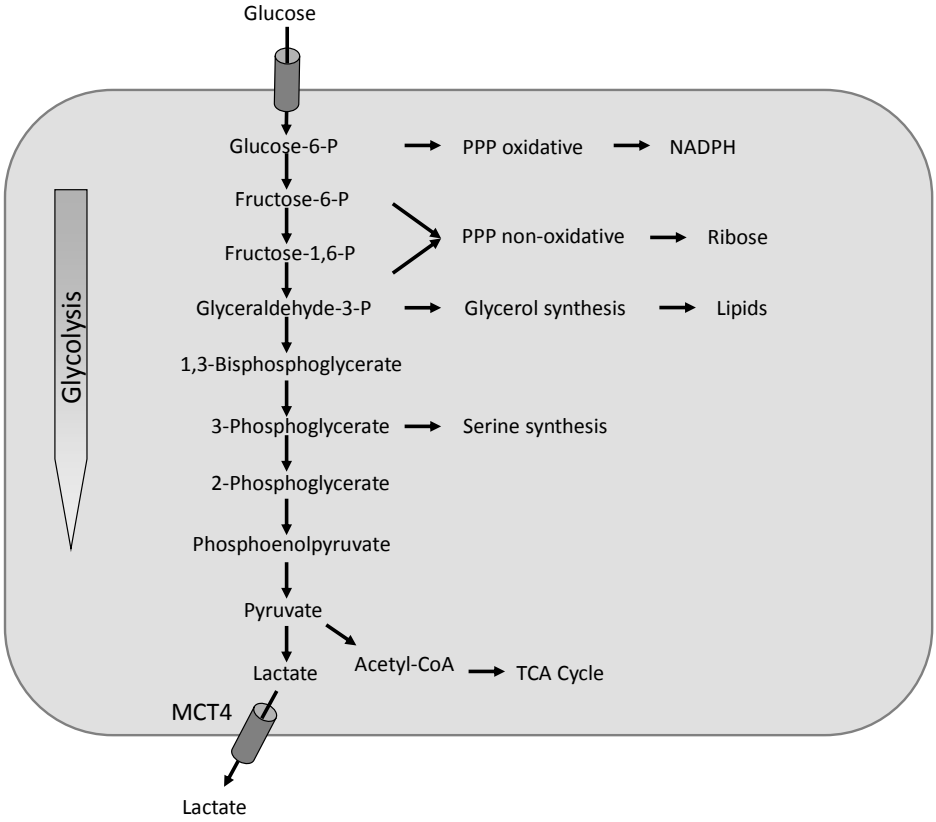

Figure 2. Reprogramming of metabolism towards biosynthetic pathways in cancer cells. In cancer cells glucose is metabolized primarily by glycolysis ("Warburg effect"), leading to excretion of large amounts of lactate, while the tricarboxylic cycle (TCA cycle, Krebs cycle) is largely bypassed, although still active.

4.4. Lactate metabolism in cancer cells

Lactate, the glycolysis end product, is known to accumulate in cancers (Fan et al., 2009; Polet and Feron, 2013). Lactate is not only a metabolic waste product but may be consumed by cancer cells, especially under low glucose concentrations. This phenomenon was described in SiHa cervix squamous cell carcinoma cancer cells (Sonveaux et al., 2008), and P53-/- HCT116 colon carcinoma cells (Boidot et al., 2012). Lactate was shown to rescue tumor cells from glucose depletion-induced death (Wu et al., 2012). It is transported into the cell via a bidirectional transporter, monocarboxylate transporter 1 (MCT1) (Halestrap, 2012) and oxidized to pyruvate via lactate dehydrogenase (Sonveaux et al., 2008), the same enzyme, that mediates the reverse reaction during glycolysis. However, the downstream metabolic pathways of lactate in cancer cells are unknown. Lactate may be oxidized to pyruvate and enter the tricarboxylic acid (TCA) cycle (Krebs cycle) via

acetyl CoA (Figure 3). Via this pathway lactate can be used by cancer cells as an energy fuel (Boidot et al., 2012; Sonveaux et al., 2008). Furthermore, acetyl CoA can be used for fatty acid (FA) synthesis (Figure 3). However, in liver cells and other gluconeogenic cells, lactate is used in the gluconeogenesis pathway to build glucose (Figure 3). Whether gluconeogenesis is present in non-hepatic cancer cells has not been clarified so far.

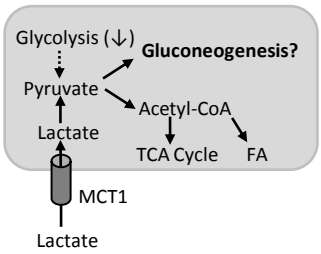

Figure 3. Potential metabolic pathways of lactate. TCA cycle, tricarboxylic acid cycle; FA, fatty acid; MCT1, monocarboxylate transporter 1;

4.5. Gluconeogenesis

Gluconeogenesis is a metabolic pathway that results in the generation of glucose from smaller carbon substrates such as lactate and amino acids (Stryer, 1995). In many aspects gluconeogenesis is the reverse of glycolysis, but differs in the requirement for phosphoenolpyruvate carboxykinase (PEPCK) and fructose-1,6-biphosphatase (FBP) (Stryer, 1995). PEPCK (EC 4.1.1.32), a key enzyme of gluconeogenesis (Xiong et al., 2011; Yang et al., 2009a), converts oxaloacetate (OAA) to phosphoenolpyruvate (PEP). Two isoforms of PEPCK exist, a cytoplasmic isoform (PCK1, PEPCK-C) and a mitochondrial isoform (PCK2, PEPCK-M). PEPCK activity is present at significant levels in the liver, but also in the kidney and in brown and white adipose tissue (Yang et al., 2009b). The factors regulating the tissue-specific expression of PEPCK and its dramatic increase in the perinatal period in the liver are poorly understood (Yang et al., 2009b). Likewise it is not known, why in fetal lungs PEPCK activitiy is almost four times as high as in adults (Engle et al., 1987).

PEPCK plays an important role in glucose formation, but also for the generation of

glycerol and serine (Kalhan and Hanson, 2012; Yang et al., 2009a). In fact, PEPCK is the bottle neck for many important biosynthetic pathways in eukaryotic cells. Still, the role of PEPCK in cancer growth is unknown. Lung cancers commonly have genetic changes associated with high glucose consumption or energy sensing, like TP53, KRAS (Kristen rat sarcoma viral oncogene), and LKB1 (lymphoma kinase B1) (Ding et al., 2008; Heist et al., 2012; Koppenol et al., 2011; Viollet et al., 2009) and typically are positive in FDG-PET (Scott et al., 1994). High glucose consumption may ultimately lead to a decrease in available glucose. Thus, we hypothesized that in lung cancer cells adaptive responses would be activated under glucose shortage, and that the gluconeogenesis pathway plays a role in this adaptation.

5. Hypothesis and specific aims

Hypothesis:
Gluconeogenesis from smaller carbon substrates, e.g. lactate serves as a metabolic rescue pathway in lung cancer cells under glucose depletion.

To test this hypothesis the following workplan was established.

Task #1: To analyze, whether the two isoforms of the key gluconeogenic enzyme PEPCK, PCK1 and PCK2, are expressed in NSCLC tissue and corresponding normal lungs using quantitative real-time PCR (qPCR) and immunohistochemistry.

Task #2: To analyze PCK1 and PCK2 expression on mRNA and protein levels in commercially available NSCLC cell lines cultured under high and low glucose conditions. Since lactate is a precursor molecule for gluconeogenesis, the impact of lactate on PCK1 and PCK2 expression was assessed.

Task #3: To clarify, whether NSCLC cells consume lactate, as potential gluconeogenic precursor, under glucose depletion.

Task #4: To analyze PEPCK activity in NSCLC cells and tissues using a biochemical assay. The specificity of this method was confirmed using a chemical PEPCK inhibitor and stable PCK2 knockdown using short hairpin RNA (shRNA). PEPCK activity was measured in cells cultured under different glucose concentrations.

Task #5. To assess the conversion of stable isotope-labelled lactate along the gluconeogenesis pathway to phosphoenolpyruvate (PEP). Using this approach, the activity of PEPCK was confirmed in intact cells. Appearance of all three labelled carbons in the PEP pool would confirm the involvement of pyruvate carboxylase, an enzyme acting up-stream of PEPCK.

Task #6: To assess the impact of PEPCK knockdown/inhibition on apoptosis and

necrosis in NSCLC cells under glucose depletion. This aim was accomplished by two different tools, one the one hand commercially available small interfering RNA (siRNA) and on the other hand by using a cell permeable specific PEPCK inhibitor (3-mercaptopicolinate, 3-MP).

Task #7: In order to understand the role of PEPCK in a cancer model mimicking the tumor microenvironment *in vivo*, multicellular spheroids from lung cancer cell lines were used. Specifically, the impact of 3-MP on the increase in spheroid size, and on apoptosis and proliferation within the spheroids was analyzed.

6. Materials and methods

6.1. Materials. Unless indicated otherwise chemicals were purchased from Sigma (St. Louis, MO). 3-mercaptopicolinic acid hydrochloride (3-MP) was purchased from AApin Chemicals (Abingdon, UK). 3-MP was diluted in water, the pH was adjusted to 7.5 with NaOH and aliquots were stored at -20°C.

6.2. Patients. NSCLC samples and corresponding normal lung tissue samples were obtained from NSCLC patients who were referred for surgery (lobectomy or bilobectomy) to the Division of Thoracic and Hyperbaric Surgery, Medical University of Graz in cooperation with the Institute of Pathology, Medical University of Graz. The study protocol was approved by the institutional ethics review board. Signed informed consent was obtained from all patients prior to surgery.

6.3. Cell lines. The human NSCLC cell lines NCI-H23 and NCI-H1299 (further referred to as H23 and H1299) were obtained from American Type Culture Collection (ATCC, Manassas, VA, USA), and were cultured in RPMI 1640 supplemented with 10% fetal bovine serum (FBS, Biowest, Nuaillé, France), 100 U/ml penicillin, and 100 µg/ml streptomycin (Gibco/Invitrogen, Carlsbad, CA, USA). The human NSCLC cell line A549 was purchased from Cell Lines Service (Eppelheim, Germany) and was cultured in DMEM-F12 culture medium (Gibco) supplemented with 10% fetal bovine serum (Biowest), 2 mM L-glutamine (Gibco), and antibiotics. HepG2 cells were purchased from Cell Lines Service and were grown in DMEM high glucose medium supplemented with 10% FBS (Biowest) and antibiotics. For passaging cells were washed with phosphate buffered saline (PBS) pH 7.4 and incubated in 0.25% Trypsin-EDTA for 5 min at 37°C. After detachment trypsin activity was stopped with serum-containing medium, and the suspension was centrifuged at 400 g for 5 min. Passaging (1:6 to 1:30) was done once to twice per week.

6.4. Low glucose cell culture. For expression analyses cells were plated onto 6-well plates or 25 cm^2 tissue culture flasks at a density of 2 $x10^4/cm^2$ and cultured in normal growth medium for one day. Thereafter cells were washed two times

with PBS and grown in DMEM or RPMI no-glucose media supplemented with different concentrations of D-glucose. L-glucose was used as osmotic balance. In case of serum supplementation, 10% dialyzed serum was used (Gibco).

6.5. Spheroids. For spheroid culture, aggregation was initiated by plating cells ($5x10^3$/well) onto ultra low-adhesion round bottom 96-well plates (Corning, Tewksbury, MA) in normal RPMI growth medium containing glutamine, supplemented with 10% FBS and antibiotics or RPMI no glucose medium containing glutamine, supplemented with 5 mM D-glucose (a physiological glucose concentration), 10% dialyzed FBS, and antibiotics. The plates were centrifuged at 1500 rpm for 10 min and thereafter cultured in a conventional CO_2 incubator. Cross-sectional areas were measured using an Olympus IX51 inverse microscope, an Olympus XC50 digital camera system and Cell^F software (Olympus, Hamburg, Germany). The volume *V* of the spheres was calculated from the cross-sectional radius *r* by the equation $V=4/3x\pi xr^3$. For immunohistochemistry spheroids were fixed and paraffin-embedded five days after plating.

6.6. Generation of cytoblocks. For the generation of cytoblocks HepG2 cells were trypsizined and centrifuged 5 min at 400 g. The pellet was resuspended in 250 µl citrate plasma containing A549 cell debris. A549 cell debris was generated from a A549 cell suspension by sonication (three times for 5 seconds) followed by centrifugation at 7200 rpm for 10 minutes. Clotting was initiated in 1.5 ml tubes (Eppendorf, Oldenburg, Germany) by adding 4 µl of a 1 M $CaCl_2$ solution. The clot was fixed in buffered formaldehyde (4%) for 24 h and paraffin embedded according to standard protocols.

6.7. Lactate analysis. For the analysis of lactate in conditioned media of NSCLC cells, cells were densely seeded into culture flasks ($1x10^7$/75 cm^2 flask). One day later cells were washed two times with PBS and incubated with serum-free media containing 10 mM L-lactate and different concentrations of D-glucose (balanced with L-glucose; 5 ml medium/flask). A small aliquot (250 µl) of medium was removed on the consecutive days for lactate analysis. Lactate was measured using the ABL800 FLEX (Radiometer A/S, Bronshoj, Denmark).

6.8. RNA extraction and cDNA synthesis. Total RNA was extracted with the Qiagen RNeasy Mini kit (Qiagen) or with the peqGOLD Total RNA Kit (PeqLab, Erlangen, Germany) according to the instructions of the manufacturer. Briefly, lysates were loaded onto a DNA removing column and centrifuged. The flow-through was mixed 1:1 with 70% ethanol and loaded onto a RNA binding column. After several washing steps RNA was eluted with 30 µl to 40 µl RNAse free water. The RNA concentration was measured on a microvolume spectrophotometer (NanoDrop 2000c, Thermo Scientific, Waltham, MA). Total RNA (1 µg) was reverse transcribed in a final volume of 20 µl using the RevertAid H Minus First Strand cDNA synthesis kit and random hexamer primers (Fermentas, Burlington, Canada) or with the iScript cDNA Synthesis Kit (BioRad Industries, Hercules, CA, USA) in a thermocycler (MyCycler, BioRad) according to the instructions of the manufacturer.

6.9. Quantitative real-time PCR (qPCR). The reactions were performed in the 7900 Real-Time PCR System (Applied Biosystems, Foster City, CA) using pre-designed TaqMan® Gene Expression Assays (Applied Biosystems) suitable for this system. Primer data are indicated in Table 1. ACTB (ß-actin) showed stable expression under our experimental conditions and was used as a reference gene. The PCR was performed in 10 µl reactions containing 1x TaqMan® Gene Expression Mastermix (Applied Biosystems), 1x TaqMan® Gene Expression Assay (Applied Biosystems) and cDNA (equal to 12.5 ng total RNA). Mean threshold cycle (Ct) number of triplicate runs were used for data analysis. Standard curves with Ct numbers on the y-axis (linear scale) and template concentration on the x-axis (logarithmic scale) were generated for every primer pair (assay). The relative expression of the gene of interest compared with the reference gene (ACTB) was calculated as $2^{\Delta Ct}$. ΔCt was calculated by subtracting the Ct number of the gene of interest from that of the reference gene.

Table 1. TaqMan® Gene Expression Assays for qPCR

Gene symbol	Gene name	Company	Assay number.	Amplicon length
PCK1	Phosphoenolpyruvate carboxykinase 1	Applied Bioysystems	Hs00159918_m1	81
PCK2	Phosphoenolpyruvate carboxykinase 2	Applied Bioysystems	Hs00388934_m1	73
ACTB	Phosphoenolpyruvate carboxykinase 2	Applied Bioysystems	Hs99999903_m1	171

6.10. Apoptosis assay. NSCLC cell lines were harvested by trypsinization and the suspension was centrifuged at 400 g for 5 min together with the floating cells. The percentage of apoptotic cells was determined with the Caspase-3 Intracellular Activity Assay Kit I (PhiPhiLux® G1D2, Merck, Darmstadt, Germany) according to the manufacturer´s protocol. Briefly, approximately $5x10^5$ cells were resuspended with 20 µl PhiPhiLux-substrate and 20 µl medium. Samples were incubated for 1 h at 37°C and washed two times with PBS prior to analysis with flow cytometry (FACS Calibur, BD Biosciences, San Jose, USA).

6.11. Necrosis assay. Propidium iodide (PI) was diluted with PBS to 1 mg/ml. From this stock a 50 µg/µl PI solution was prepared. Cells were plated into 6-well plates and treated as indicated. After trypsinization, the suspension was centrifuged at 400 g for 5 min together with the floating cells. The pellet was resuspended in 200 µl PBS and 6 µl of the 50 µg/µl PI solution was added. After incubation for 5 min at room temperature in the dark, the percentage of PI positive cells was determined using flow cytometry (FACS Calibur, BD Biosciences). PI enters cells with a damaged cell membrane (necrotic cells and late apoptotic cells) which show red fluorescence, while viable or apoptotic cells do not take up PI.

Table 2. Primary antibodies

Antigen	Species/mono-clonal or polyclonal	Company (clone)	Cat.-No.	Dilution	Incub-ation/ solvent	Application
Cleaved caspase 3	Rabbit polyclonal	R & D	AF835	1:200	1 h rt/IHC dilution buffer	IHC
PCK2	Rabbit polyconal	Abcam	ab137580	1:200	1.5 h rt/ IHC dilution buffer	IHC
PCK1	Mouse monoclonal	Abcam	ab55509	1:50	1.5 h rt/ IHC dilution buffer	IHC
PCK2	Mouse monoclonal	Abcam	ab77047	1:500	1.5 h rt/ 5% BSA	Western blot
PC	Rabbit polyclonal	Santa Cruz (H-300)	sc-67021	1:500	overnight 4°C/ 5% milk	Western blot
Beta-actin	Mouse monoclonal	Santa Cruz (C4)	sc-47778	1:3000	1 h rt/ 5% BSA	Western blot

IHC, immunohistochemistry; BSA, bovine serum albumin, rt, room temperature.

6.12. Immunohistochemistry. Serial sections of paraffin-embedded spheroids were deparaffinized and rehydrated according to standard protocols. A rabbit polyclonal antibody against human/mouse cleaved caspase 3 (R&D Systems, Minneapolis, MN) was diluted in PBS pH 7.4 containing 0.1% BSA (Carl Roth, Karlsruhe, Germany) and 0.1% Tween 20 (Sigma) (IHC dilution buffer) and applied as indicated in Table 2. PCK2 immunohistochemistry was performed with a rabbit polyclonal PCK2 antibody (Abcam, Cambridge, MA, USA), diluted in IHC dilution buffer as indicated in Table 2. The primary antibodies were detected with the Ultravision LP detection system (Thermo Scientific, Waltham, MA). Peroxidase activity was visualized by incubation with 3-amino-9-ethylcarbazole solution (Dako, Glostrup, Denmark). As a negative control, a rabbit isotype control primary antibody was used at the same concentration as the cleaved caspase-3 or PCK2 antibody.

6.13. Evaluation of immunohistochemistry. For evaluation of apoptosis and mitosis rates, images of the largest section of each spheroid (the section closest to the center of the spheroid) were taken using an Olympus BX51 microscope, a DP12 digital camera system and Cell^D software (Olympus, Hamburg, Germany). The percentage of caspase-3 positive cells and cells showing mitotic figures were determined from the entire spheroid section. At least 5 spheroids were evaluated per treatment in each experiment. In the case of PCK2 immunohistochemistry all of the sections were examined by a thoracic pathologist (Dr. Elvira Stacher-Priehse) at x400 magnification using a Zeiss Axioplan 2 microscope (Oberkochen, Germany) and evaluated essentially as described previously (Kothmaier et al., 2008). Staining scores were calculated by multiplying the percentage of positive cells by the staining intensity.

6.14. In silico gene expression analysis. Expression values for MCT1 and MCT2 were obtained from a lung cancer dataset, GDS3257, published at Gene Expression Omnibus (GEO; http://www.ncbi.nlm.nih.gov/geo/). Details on microarray processing and patient characteristics are reported at GEO and in (Landi et al., 2008).

6.15. Western blot. Cells were lysed on ice in Ripa buffer (Sigma) containing protease inhibitor and homogenized two times for two seconds using a sonicator. Insoluble material was removed by centrigugation (13.000 rpm for 15 min). The protein concentration in the supernatant was determined using a BCA kit (Novagen, Darmstadt, Germany). 20 µg protein was incubated at 95°C for 10 min in Leammli buffer, loaded onto a 10% acrylamide gel, separated by sodium dodecyl sulfate-polyacrylamide gel electrophoresis using the Mini-PROTEAN® electrophoresis unit (Bio-Rad), and transferred to a PVDF membrane (Bio-Rad). Prior to immunostaining the membrane was blocked with TBS buffer containing 0.1% Tween 20 (Sigma) and 5% dry milk for one hour at room temperature. The following antibodies were used: monoclonal mouse antibody to PCK2 (Abcam, ab77047, Table 2), polyclonal rabbit antibody to pyruvate carboxylase (Santa Cruz, H-300, Table 2). Antibodies were either diluted in TBS buffer containing 0.1% Tween 20 (TBST) and 5% milk (PC) or in TBST containing 5% bovine serum

albumin (PCK2). As secondary antibodies rabbit IgG antibodies or mouse IgG antibodies conjugated to horseradish peroxidase were used. Peroxidase activity was detected using chemiluminescence detection (ECL Prime, GE Healthcare, Uppsala, Sweden or SuperSignal West Pico Chemisluminescent Substrate, Thermo Scientific). As a loading control, membranes were stripped using Restore PLUS Western Blot Stripping Buffer (Thermo Scientific) according to the manufacturer´s instructions and stained with a polyclonal antibody to β-actin (Santa Cruz, Table 2).

6.16. Knockdown of PCK2 by siRNA. siRNA targeting PCK2 was obtained from Santa Cruz Biotechnology (Santa Cruz, CA, USA). Transfection was performed at a final concentration of 40 nM siRNA using Effectene (Qiagen, Hilden, Germany) according to the manufacturer´s instructions. The efficacy was assessed 48 h after transfection by qPCR and Western blot.

6.17. Stable expression of shRNA targeting PCK2. Stably short hairpin RNA (shRNA) expressing cells were generated by transfection with four different commercially available shRNA plasmids targeting PCK2 or a non-silencing control shRNA (Qiagen) followed by puromycin selection with 1.5 µg/ml puromycin (Sigma) for two weeks. Thereafter cells were cultured in media containing a reduced puromycin concentration (0.75 µg/ml). The sub-cell lines with greatest PCK2 reduction were used for further analysis. The most effective shRNA sequences were as follows: A549 cells: AACCCTGAGAACGGCTTCTTT; H1299 cells: AGCAAGACGGTGATTGTAACT. Puromycin was omitted during the course of the experiments.

6.18. PEPCK activity assay. 5.2 x 10^6 cells were seeded into 75 cm^2 flasks. One day later cells were washed two times with PBS and grown in DMEM or RPMI serum-free no-glucose media supplemented with 10 mM L-lactate and 1 mM D-glucose for the indicated times. If low glucose conditions were compared to high glucose conditions, D-glucose was balanced with L-glucose. Cells were washed with PBS, scraped and centrifuged. The pellet was resuspended in 250 µl of ice-cold isolation buffer [10 mM Hepes pH 7.4, 250 mM sucrose, 1 mM EDTA, 1 mM dithiothreitol]. Mouse liver and human NSCLC tissue were homogenized in

isolation buffer using a VDI12 homogenizer (VWR, Radnor, PA, USA) Both, homogenates and suspensions, were then sonicated with three 5 sec pulses and centrifuged at 5000 g for 10 min. The protein concentration was determined in the supernatants using a BCA kit (Novagen). A continuous enzymatic assay was used to measure PEPCK activity in the supernatants, in which OAA produced by PEPCK is immediately reduced to malate in a coupled assay with malate dehydrogenase exactly as described (Stark et al., 2009). The reactions were performed in triplicates in 96-well plates (Nunclon Delta Black Microwell SI, Nunc A/S, Roskilde, Denmark) with a final volume of 200 µl containing 110 mM imidazole-Cl, pH 6.8, 3 mM $MnCl_2$, 13 mM NaF, 10 mM phenylalanine, 1 µM rotenone, 30 mM $NaHCO_3$, 0.15 mM NADH, 6 units/ml malate dehydrogenase, 2 mM phosphoenolpyruvate, and cell homogenate containing 25 to 100 µg of protein. The reactions mixture was prepared using stock solutions prepared (Table 3). All stock solutions were stored in aliquots at -20°C. Reactions mixtures were freshly prepared from the stock solutions. Before the experiment the reaction mixture was gassed with 100% CO_2 for 15 min. The reaction was initiated with 0.5 mM dGDP. The oxidation of NADH (nicotinamide adenine dinucleotide) by malate dehydrogenase was measured at 355 nm for excitation and 460 nm for emission every 80 sec for 45 min using the FluoStar OPTIMA microplate reader (BMG Labtech, Ortenberg, Germany) and MARS Data Analysis Software version 1.0 (BMG Labtech). Control samples lacking HCO_3^-/CO_2 were run simultaneously and this background NADH consumption was subtracted from the consumption in the complete reaction. One unit of PEPCK activity corresponds to the production of 1 µmol product min^{-1} at 37°C.

Table 3. Stock solutions for PEPCK activity assay

Substance	MW	Final assay concentration	Stock concentration	Amount [mg]	Total Volume	Aliquots [µl]
Imidazole-Cl pH 6.8	68.08	110 mM	250 mM	851	50 ml	-
MnCl2*4H2O	197.91	3 mM	100 mM	99	5 ml	300
NaF	41.99	13 mM	500 mM	105	5 ml	300
Phenylalanine	165.2	10 mM	100 mM	330.4	20 ml	900
Rotenone	394.4	1 µM	1 mM	7.9	20 ml	200
PEP	168.04	2 mM	100 mM	67.2	4 ml	200
NaHCO3	84.01	30 mM	500 mM	210	5 ml	250
dGDP	427.2	0.5 mM	5 mM	25	11.8 ml	500
NADH	741.62	0.15 mM	20 mM	35.52	2400 µl	120

PEP, phosphoenolpyruvate.

6.19. LC-MS/MS analysis of phosphoenolpyruvate (PEP). LC-MS/MS was performed by Dr. Harald Köfeler, Dr. Martin Trötzmüller, and Astrid Knopf, Core Facility Mass Spectrometry at the Center for Medical Research (CMR, ZMF), Medical University of Graz. Cells were plated into 75 cm^2 flasks ($2x10^6$ cells per flask), pre-treated in low glucose medium for the indicated times, and incubated in 5 ml serum-free DMEM or RPMI medium containing 1 mM D-glucose and 5 or 10 mM $^{13}C_3$-lactate or lactate for 12 h. Thereafter cells were washed with glucose free media, and extracted with ice-cold methanol (1 ml per flask) using a scaper. The lysate was sonicated three times for 10 sec on ice, transferred to glas tubes, and centrifuged. The supernatant was analyzed by a 4000QTrap mass spectrometer (AB Sciex, Toronto, Canada) coupled to an Agilent 1100 HPLC system (Santa Clara, CA). Chromatography was done on a Thermo Hypersil column with a binary water – acetonitrile gradient. PEP and $^{13}C_3$- PEP were monitored in negative electrospray ionization mode by multiple reaction monitoring of characteristic fragment m/z 79 (phosphate). Areas of labelled and non-labelled PEP were determined and compared. The $^{13}C_1$ derived M+1 peak of glyceraldehyde-3-phosphate (GA-3-P) at m/z 170 accounts for 3.3% of the deprotonated GA-3-P M molecular ion at m/z 169 and was subtracted in an isotopic correction step from the isobaric $^{13}C_3$-PEP signal at m/z 170.

6.20. Statistical analysis. The data were compiled and analyzed with the software package SPSS, version 20.0 (Chicago, IL). Group differences were calculated using Wilcoxon signed-rank test, Two-way ANOVA, One-Way ANOVA with Tukey post-hoc analysis, and paired or unpaired Student´s t-test as appropriate. *P*-values smaller than 0.05 were considered significant.

7. Results

7.1. Direction of lactate transport in lung cancer cells.

First we clarified whether lactate is consumed under low glucose conditions in three lung cancer cell lines, A549, H23 and H1299. Cells were cultured in serum-free medium containing lactate (10 mM) in the presence of either 20 mM glucose or 1 mM glucose. As expected, in high glucose (20 mM) media a net production of lactate by NSCLC cells was found (Figure 4*A*). In contrast, under a low glucose concentration (1 mM), lactate was significantly consumed, as evidenced by a decline in lactate levels in the medium (Figure 4*A*).

Then we analyzed whether the transporter responsible for lactate import is expressed in a panel of human lung cancers. The monocarboxylate transporter MCT1 mediates both, import and export of lactate and other monocarboxylates. In contrast, MCT4 is highly expressed in glycolytic tissues and is believed to preferentially mediate export of lactate (Halestrap, 2012). We assessed expression levels of MCT1 and MCT4 in NSCLCs from a large dataset (Landi et al., 2008) published at GEO (GDS3257). Both, MCT1 and MCT4 were overexpressed in lung cancer samples compared to corresponding normal lungs (Figure 4*B*).

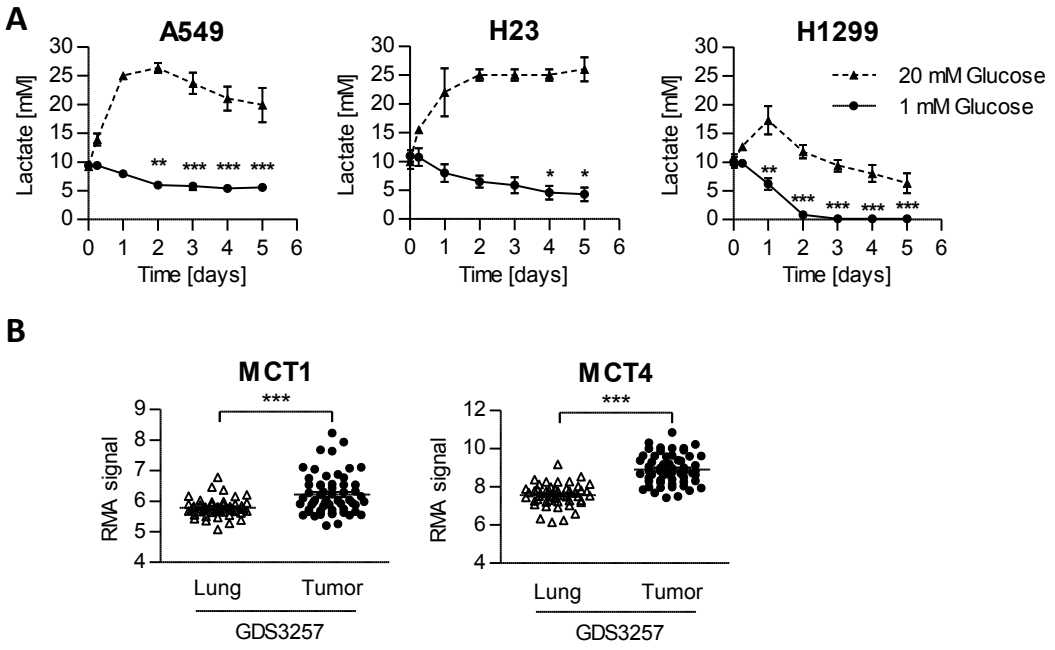

Figure 4. Direction of lactate transport in lung cancer cells. (**A**) Human NSCLC cells were densely seeded into culture flasks. One day later cells were washed two times with PBS and incubated with serum-free media containing 10 mM L-lactate and different concentrations of D-glucose. Results are mean +/- SEM from three independent experiments. (**B**) mRNA levels of MCT1 and MCT4 were assessed in a publically available GEO dataset (GDS3257) in lung adenocarcinoma samples (n=58) and normal lungs (n=49). * *P*<0.05; ** *P*<0.01, *** *P*<0.001. TCA cycle, tricarboxylic acid cycle; FA, fatty acid; MCT1, monocarboxylate transporter 1; MCT4, monocarboxylate transporter 4; RMA, Robust Multichip Average.

7.2. PCK2 is expressed in NSCLC samples and NSCLC cells.

Next we explored whether PEPCK is expressed in lung cancer. To this end we assessed levels of PCK1 and PCK2 mRNA in surgically removed tumor tissue from NSCLC patients and corresponding normal lungs. PCK2, the mitochondrial isoform of PEPCK, was significantly overexpressed in tumor tissue (Figure 5*A*). PCK1, the cytoplasmic isoform of PEPCK, was expressed only at very low levels in both, tumor tissue and normal lung (Figure 5*A*). PCK2 protein expression was evaluated in NSCLC samples using immunohistochemistry. For the establishment of PCK2 immunostaining, cytoblocks of HepG2 cells were generated, since HepG2 cells are known to express PCK2 (Goldstein et al., 2013). Figure 6 shows a positive peroxidase reaction in HepG2 cells stained with a PCK2 antibody, while the isotype control with non-immune antibodies was negative.

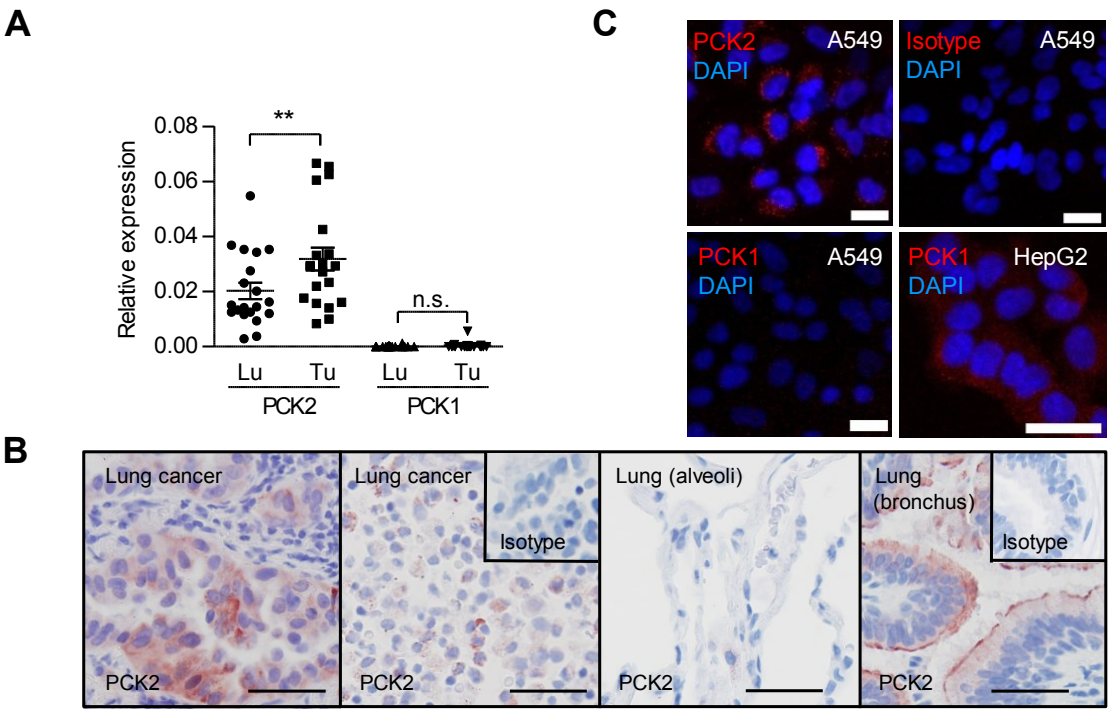

Figure 5. Expression of the gluconeogenic key enzyme PCK2 in lung cancer cells. (**A**) PCK1 and PCK2 mRNA levels were measured by qPCR in NSCLC samples and corresponding normal lungs from 19 patients. Mean threshold cycle (Ct) number of triplicate runs were used for data analysis. The relative expression of the gene of interest compared with the reference gene (ß-actin) was calculated as $2^{\Delta Ct}$. ΔCt was calculated by subtracting the Ct number of the gene of interest from that of the reference gene. (**B**) PCK2 immunohistochemistry in lung cancer samples and corresponding normal lung tissue. Two examples of positive PCK2 immunostaining in lung cancer are shown. Normal pneumocytes (alveolar cells) were PCK2 negative, while the respiratory epithelium (bronchial epithelium) was positive. Scale bar: 50µm. (**C**) PCK1 and PCK2 immunofluorescence in A549 cells. HepG2 liver carcinoma cells served as a positive control for PCK1. HepG2 cells were purchased from Cell Lines Service and were grown in DMEM high glucose medium supplemented with 10% fetal calf serum (Biowest) and antibiotics. Scale bar: 20µm. ** *P*<0.01. PCK1, cytoplasmic isoform of phosphoenolpyruvate carboxykinase; PCK2, mitochondrial isoform of phosphoenolpyruvate carboxykinase; Lu, lung; Tu, tumor.

Lung cancer and normal lung tissue were stained for PCK2 by immunohistochemistry and staining was evaluated by a thoracic pathologist (Dr. Elvira Stacher-Priehse, Institute of Pathology, Medical University of Graz). We found PCK2 immunoreactivity in tumor cells in 14/20 patients (70%) at variable percentages (1-90% of tumor cells, Figure 5*B*). In the normal corresponding lung alveolar cells were PCK2 negative, while the bronchial epithelium was positive (Figure 5*B*).

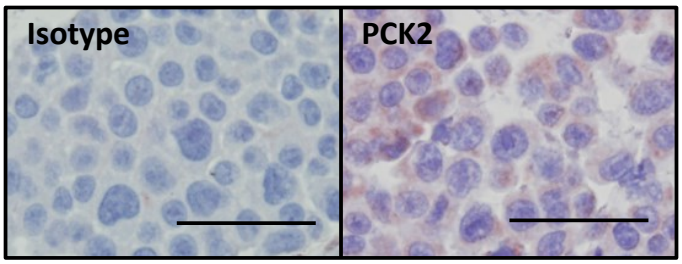

Figure 6. Establishment of PCK2 immunohistochemistry. For the establishment of PCK2 immunohistochemistry HepG2 cells were incorporated into cellblocks. A rabbit isotype antibody (left) was used to exclude non-specific staining.

Examining the expression of PCK1 and PCK2 in A549 lung cancer cells by immunofluorescence, we found a positive staining for PCK2, while A549 cells were negative for PCK1 (Figure 5*C*). Using Western blot we confirmed the presence of PCK2 protein in A549 cells. When the cells were cultured under different glucose concentrations for 48 h, a modulation of PCK2 expression by glucose was found, with a peak expression of PCK2 at 1 mM glucose (Figure 7). Supplementation with L-lactate had no effect on PCK2 expression (Figure 7).

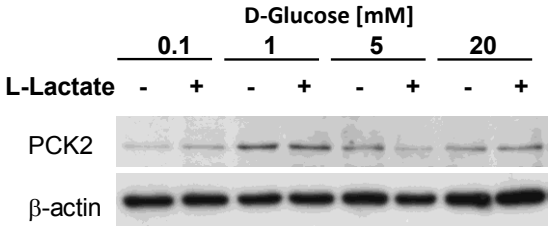

Figure 7. Effect of glucose and lactate on PCK2 expression in A549 cells. A549 cells were grown for 48 h in culture media containing different concentrations of D-glucose with or without 10 mM L-Lactate. A representative PCK2 immunoblot is shown. Beta-actin served as a loading control. PCK2, mitochondrial isoform of phosphoenolpyruvate carboxykinase.

Pyruvate carboxylase (PC) is an important gluconeogenic enzyme acting up-stream of PEPCK (Stryer, 1995). PC converts pyruvate to OAA, which is further metabolized by PEPCK. PCK2 and PC were analyzed using Western blot on the protein level at 1 mM glucose in comparison to 20 mM glucose in all three lung cancer cell lines. The experiments were performed in both, serum-free and serum-

containing media. Serum contains lipids and thus glycerol, which is a possible gluconeogenic precursor. Thus serum may potentially affect the expression and function of gluconeogenesis enzymes. PCK2 and PC were expressed in all three cell lines (Figure 8*A*,*B*). We found that PCK2 expression was enhanced under low glucose conditions (Figure 8*A*,*B*). The differences between low and high glucose were significant in A549 cells and H1299 cells in both serum-free and serum-containing media (10% serum), and in H23 cells in medium containing 10% serum (Figure 8*A*,*B*). Again, supplementation with L-lactate had no effect on PCK2 expression. PC was found to be constitutively expressed in all three cell lines, however, at different levels (Figure 8*A*,*B*).

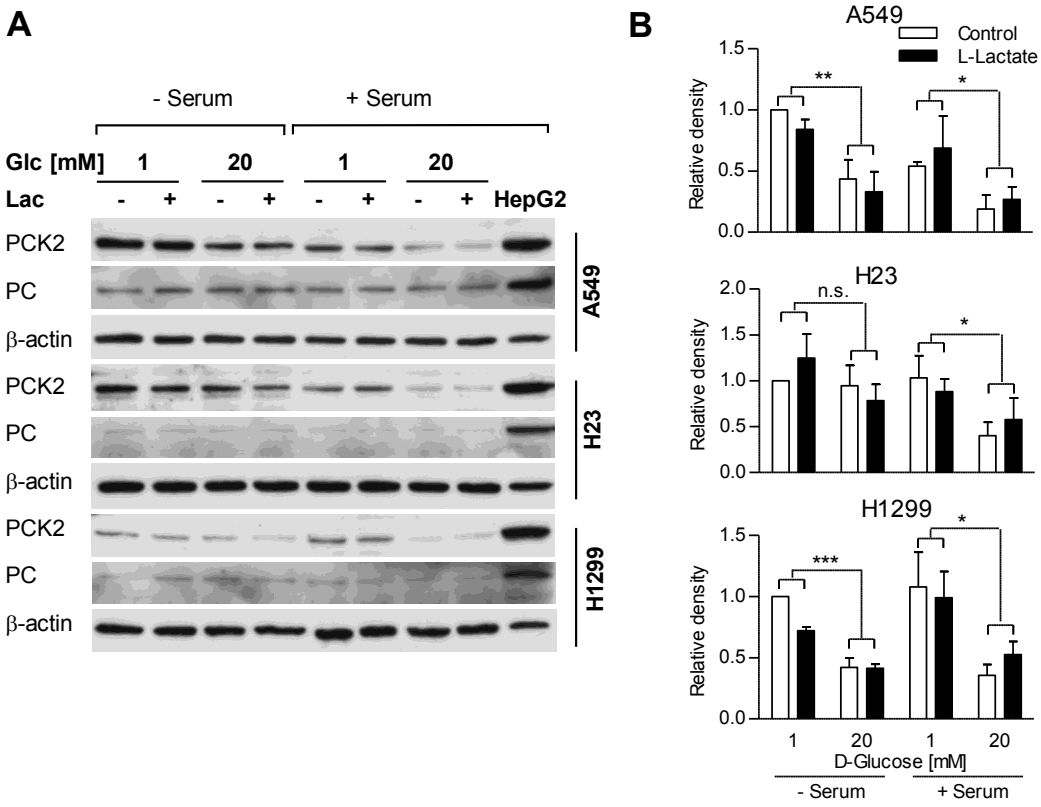

Figure 8. Expression of PCK2 and PC in lung cancer cell lines. (**A,B**) PCK2 and PC expression in three different NSCLC cell lines incubated with media containing different concentrations of D-glucose and 0 mM or 10 mM L-lactate for 48 h. In case of serum supplementation, 10% dialyzed serum was used. Representative immunoblots (**A**) and mean densitometry values normalized to untreated cells +/- SEM from n=3 to 4 independent experiments (**B**) are shown. Group differences were calculated using Two-Way ANOVA. * $P<0.05$, ** $P<0.01$, *** $P<0.001$. PCK1, cytoplasmic isoform of phosphoenolpyruvate carboxykinase; PCK2, mitochondrial isoform of phosphoenolpyruvate carboxykinase; PC, pyruvate carboxylase; Glc, D-glucose; Lac, L-lactate.

7.3. PEPCK activity is enhanced in tumors compared to normal lungs.

A conventional PEPCK assay was used to assess whether PEPCK is functional in NSCLC samples and NSCLC cells (Stark et al., 2009). PEPCK activity was measured in archival liquid nitrogen frozen NSCLC tissue and corresponding normal lung tissue from patients (n=19) treated with surgery. The mean PEPCK activity in tumor samples was three times as high as in lungs (0.84 mU/mg protein versus 0.28 mU/mg protein; *P*= 0,00038; Figure 9*A*).

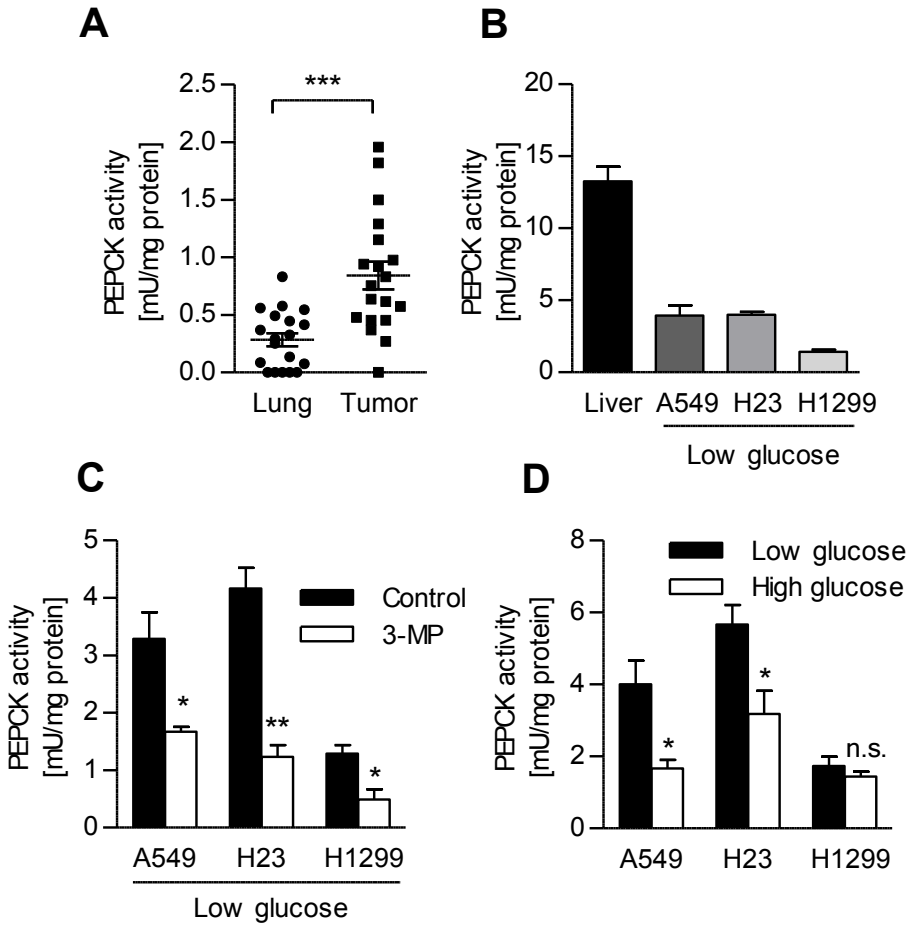

Figure 9. PEPCK activity in lung cancer cells. (**A**) PEPCK activity was measured in 19 samples of of archival liquid nitrogen frozen NSCLC and corresponding normal lungs and normalized to total protein. Lines are mean +/- SEM. (**B**) Lung cancer cells were allowed to adapt to glucose starvation by incubation for three days in serum-free media containing 1 mM D-glucose and 10 mM L-lactate. PEPCK activity normalized to total protein was measured in total cell lysates. Lysate of overnight-starved mouse liver served as a positive control. (**C**) Lysates of low glucose-treated cells were incubated with the PEPCK inhibitor 3-mercaptopicolinate prior to analysis. (**D**) Lung cancer cells were cultured for three days in serum-free media containing 20 mM D-glucose and 10 mM L-lactate or 1 mM D-glucose and 10 mM L-lactate. All activity results are mean +/- SEM from n=3-4 independent experiments. * *P*<0.05, ** *P*<0.01, *** *P*<0.001.

7.4. PCK2 is active in NSCLC cells under low glucose conditions.

NSCLC cells were allowed to adapt to low glucose conditions in a serum-free medium for three days (scheme in Figure 10). After low glucose high lactate treatment, A549 and H23 cells were found to possess mean PEPCK activities of app. 4 mU/mg protein which was 30% of starved mouse liver lysates used as a positive control (Figure 9*B*). In H1299 cells the PEPCK activity was lower (1.4 mU/mg protein). Incubation of lysates with the PEPCK inhibitor 3-mercaptopicolinate (3-MP; 1 mM) (Makinen and Nowak, 1983) significantly reduced PEPCK activity (Figure 9*C*). PEPCK activities were significantly reduced in A549 and H23 cells, but not in H1299 cells, if cells were incubated for three days in medium containing high glucose (20 mM) in comparison to low glucose (1 mM; Figure 9*D*).

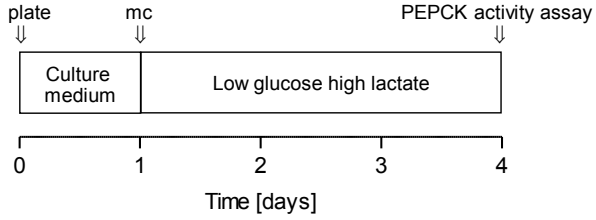

Figure 10. Experimental protocol for PEPCK activity assay. For all PEPCK activity tests lung cancer cells were allowed to adapt to glucose starvation by incubation for three days in serum-free media containing 1 mM D-glucose and 10 mM L-lactate. Thereafter cells were scraped and PEPCK activity was measured using a coupled enzymatic assay. mc, medium change. PEPCK, phosphoenolpyruvate carboxykinase.

To confirm the contribution of the PCK2 isoform to the measured PEPCK activities in NSCLC cell lines we used a commercially available PCK2 shRNA. PCK2 shRNA or control shRNA expressing cells were selected using puromycin selection. The knockdown of PCK2 in cells stably expressing PCK2 shRNA was effective, as shown by qPCR (Figure 11*A*). We found that PEPCK activity was significantly lower in cells stably expressing PCK2 shRNA (Figure 11*B*).

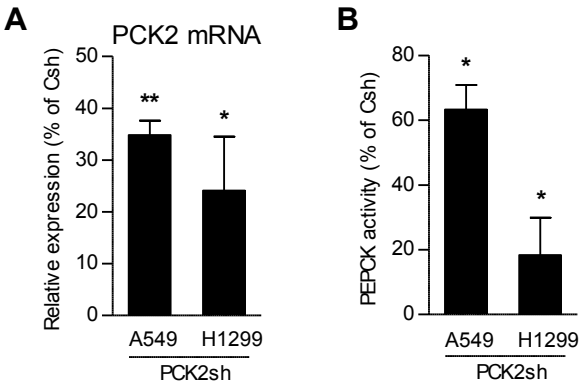

Figure 11. PEPCK activity in lung cancer cells stably expressing PCK2 shRNA. Cells with stable PCK2 shRNA expression were generated by transfection with four different commercially available shRNA plasmids targeting PCK2 or a non-silencing control shRNA (Qiagen) followed by selection with puromycin. The sub-celllines with greatest PCK2 reduction were used for further analysis. (**A**) Relative levels of PCK2 mRNA in cells treated for two days with medium containing 1mM glucose are shown. (**B**) Relative PEPCK activity in stably PCK2 shRNA and control shRNA expressing cells treated as described in Figure 10. Results are mean +/- SEM from three to four independent experiments. * P<0.05., ** P<0.01. Csh, control shRNA, Psh, PCK2 shRNA.

7.5. Stable isotope analysis of the gluconeogenesis pathway in lung cancer cells.

Stable isotope analysis was used to assess whether a metabolic flux from lactate to phosphoenolpyruvate via PEPCK occurs in NSCLC cells in steady state experiments. The hypothetical metabolic pathway is shown in Figure 13*A*. A549, H23 and H1299 cells were allowed to adapt to low glucose high lactate conditions (1 mM D-glucose and 10 mM L-lactate in serum depleted medium) for 60 h (Figure 12). Thereafter lactate was replaced by $^{13}C_3$-labelled lactate and cells were grown for additional 12 h.

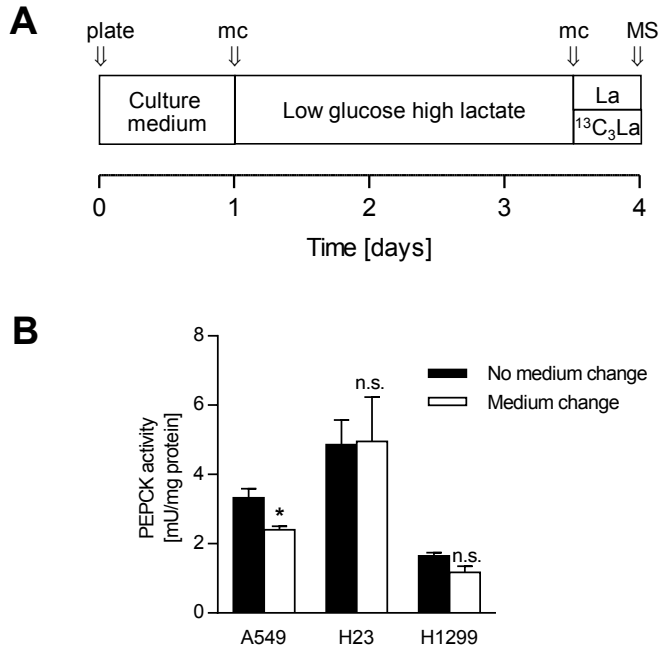

Figure 12. Experimental protocols for stable isotope experiments and their impact on PEPCK activity. (**A**) Stable isotope experiments were designed in a fashion allowing steady state conditions and avoiding a depletion of labelled lactate. To this end, cells were allowed to adapt to glucose starvation by incubation for 60 h in serum-free media containing 1 mM D-glucose and 10 mM L-lactate. Then lactate was replaced by $^{13}C_3$-labelled lactate in half of the samples and cells were grown for additional 12 h. (**B**) PEPCK activity under the conditions described in (**A**) and in conventional experiments without medium change. Results are mean +/- SEM from n=3 independent experiments.

$^{13}C_3$-PEP was detectable in all NSCLC cell lines treated with $^{13}C_3$-lactate, whereas only a small background peak was detectable in cells treated with unlabelled lactate (Figure 13*B*), indicating that the conversion of $^{13}C_3$-lactate along the depicted pathway occurred. The medium replacement necessary to switch from lactate to $^{13}C_3$-lactate, slightly reduced PEPCK activities in A549 cells (Figure 12), still PEPCK activity was clearly measurable.

In the presence of the PEPCK inhibitor 3-MP the ratio of labelled PEP to unlabelled PEP was significantly reduced at two different concentrations of $^{13}C_3$-lactate (Figure 13*C*). When A549 cells with stable expression of PCK2 shRNA were incubated with $^{13}C_3$-labelled we could not observe a reduction in $^{13}C_3$-PEP accumulation compared to A549 cells stably expressing a control plasmid (Figure 13*D*).

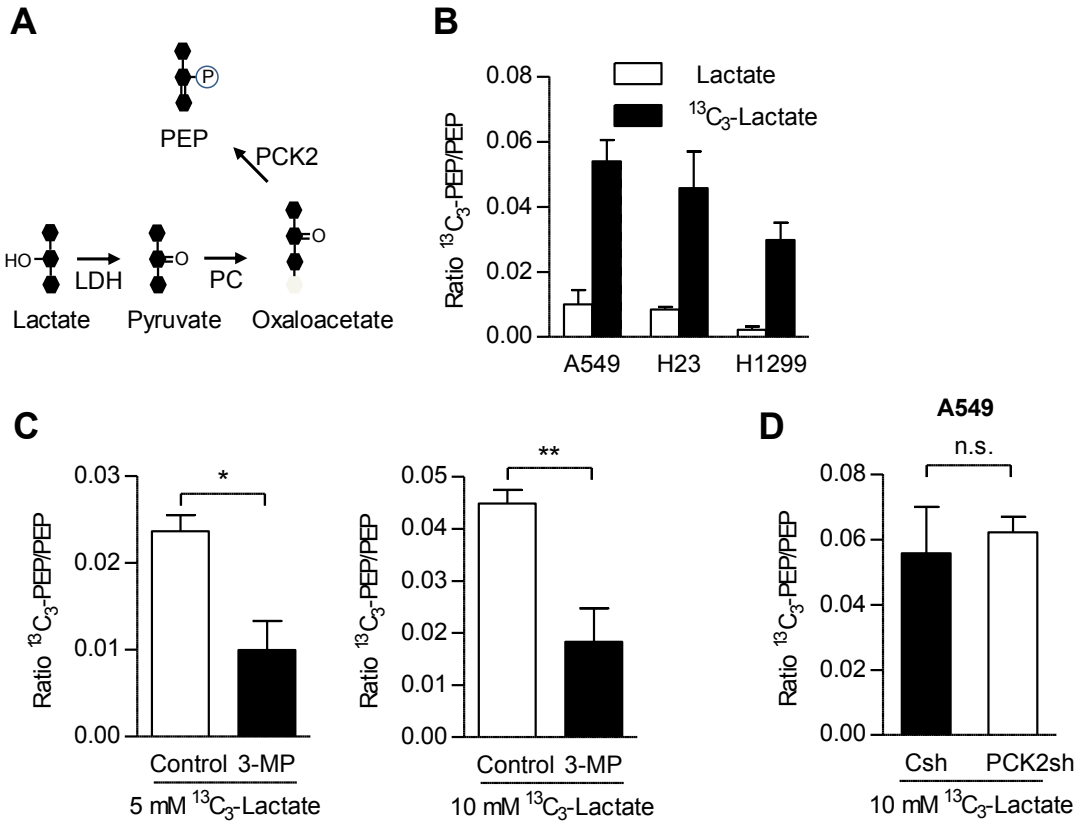

Figure 13. Assessment of conversion of $^{13}C_3$-lactate to $^{13}C_3$-phosphoenolpyruvate (PEP) as a proof of PEPCK activity. (**A**) Hypothetical metabolic pathway leading to PEP generation from lactate via pyruvate carboxylase (PC). (**B**) The ^{13}C label appeared in all three carbons of PEP in $^{13}C_3$-lactate (5 mM) treated cells. In contrast, only background signals were present in cells treated with non-labelled lactate. PEP and the M+3 isotopomer were measured using LC-MS/MS. (**C**) Pretreatment with 1 mM 3-MP was performed for 5 h. $^{13}C_3$-lactate was administered at 5 mM or 10 mM for 12 h in the presence or absence of 3-MP. (**D**) $^{13}C_3$-PEP accumulation in stably shRNA expressing cells. Values are mean +/- SEM from four independent experiments. * P<0.05, ** P<0.01. 3-MP, 3-mercaptopicolinate.

7.6. Inhibition of PCK2 enhances glucose depletion-induced apoptosis and reduces growth of multicellular spheroids. NSCLC cells adapted to 1 mM glucose (Figure 14), however, severe glucose depletion (0.2 mM) led to the induction of cell death. Thus, we used culture medium containing 0.2 mM glucose to analyze the impact of PCK2 on cell survival under very low glucose conditions.

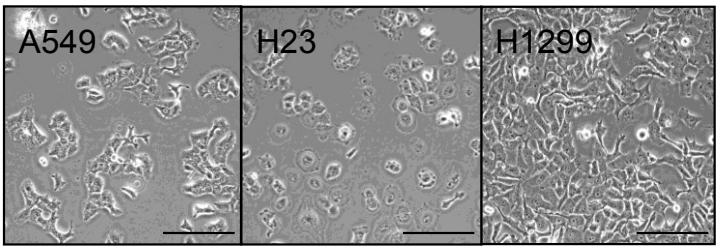

Figure 14. NSCLC cells adapt to 1 mM glucose. Morphological appearance of NSCLC cells cultured in serum-free media containing 1 mM D-glucose and 10 mM L-lactate for three days. Scale bar: 100 µm.

Transfection with PCK2 siRNA resulted in the reduction of PCK2 (Figure 15*D*). PCK2 siRNA led to a significant increase in glucose depletion-induced apoptosis in A549 and H23 cells, while in H1299 only an insignificant, mild effect was found (Figure 15*A*). On the other hand under high glucose conditions PCK2 siRNA had no effect (Figure 15*A*). When necrosis/late apoptosis was assessed using a propidium iodide exclusion assay, a similar but less pronounced increase was found with PCK2 siRNA under low glucose (Figure 15*B*), indicating that PCK2 primarily protects from apoptosis. The increase in cell death with PCK2 siRNA under low glucose was also evident from the morphological appearance of the cells, with many floating cells under 0.2 mM glucose in combination with PCK2 siRNA treatment, as opposed to treatment with control siRNA (Figure 15*C*).

Similar to PCK2 siRNA, treatment with the PEPCK inhibitor 3-MP led to a significant increase in glucose depletion-induced apoptosis in A549 and H23 cells, while in H1299 only an insignificant, mild effect was found (Figure 16). On the other hand, under high glucose conditions 3-MP had no effect (Figure 16).

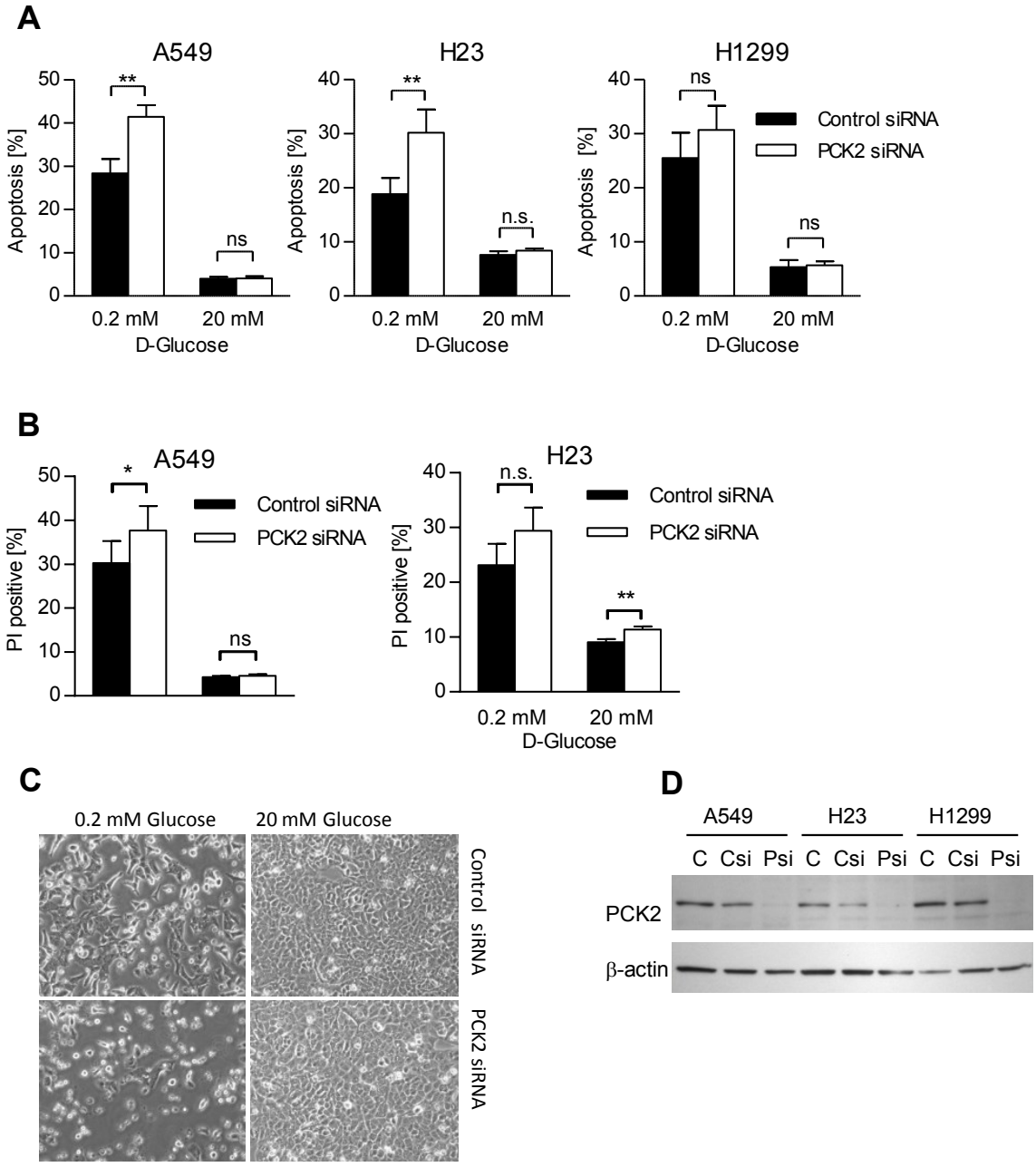

Figure 15. Impact of PCK2 siRNA on lung cancer cell death. (**A**) Apoptosis was measured in A549, H23, and H1299 cells transfected with control siRNA or PCK2 siRNA (a pool of three different siRNAs), incubated for one day in normal growth medium, and treated for additional three days with high or low glucose containing medium supplemented with 10mM L-lactate without serum (n=4 independent experiments). Results are mean +/- SEM. Group comparisons were performed with Two-Way ANOVA followed by post-hoc analysis. (**B**) Alternatively cell death was analyzed with a propidium iodide exclusion assay. Group comparisons were performed with paired Student´s t-test. Results are mean +/- SEM. (**C**) Morphological appearance of A549 cells treated as in panel (**A**) and (**B**). (**D**) The efficacy of PCK2 siRNA transfection was assessed 48 h after transfection. A representative immunoblot for PCK2 two days after transfection with PCK2 siRNA is shown. C, control; Csi, non-silencing siRNA; Psi; siRNA targeting PCK2; PI, propidium iodide. * P<0.05, ** P<0.01.

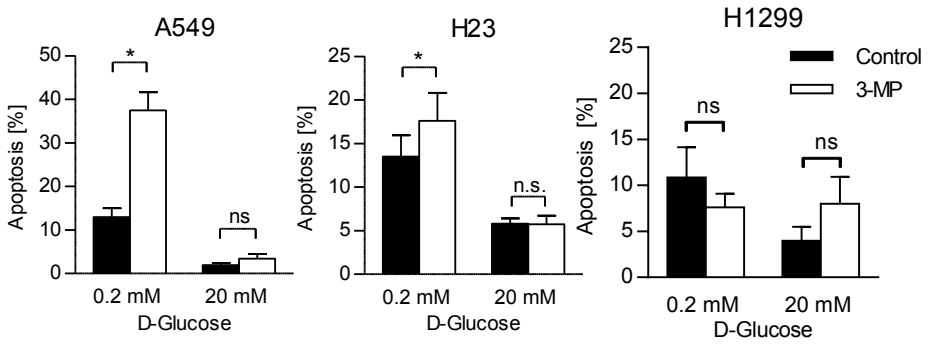

Figure 16. Impact of PEPCK inhibitor 3-mercaptopicolinate on lung cancer cell death. Cells were preincubated for 5 h with the PEPCK inhibitor 3-mercaptopicolinate (1 mM) or vehicle (H_2O). Thereafter high or low glucose media were added as described above, either containing 3-MP or vehicle (Control). After three days of treatment, apoptosis was assessed with the PhiPhiLux assay. Results are mean +/- SEM. Group comparisons were performed with paired Student´s t-test. * *P*<0.05.

Multicellular spheroids serve as a 3D cancer model which mimics the metabolic microenvironment of cancers in vivo (Hirschhaeuser et al., 2010). Inside such spheroids gradients for nutrients and oxygen occur (Hirschhaeuser et al., 2010). The NSCLC cell lines were screened for the ability to grow as multicellular spheroids. H23 spheroids exhibited a typical spheroid morphology and measurable growth between day 3 and day 6 after plating (Figure 17). Thus, all experiments were performed with H23 spheroids.

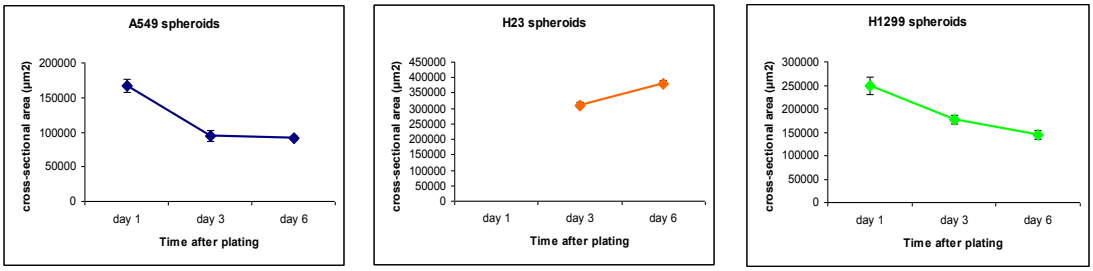

Figure 17. Assessment of the ability of cancer cells lines to growth as multicellular spheroids. Aggregation of A549, H23, and H1299 cells into spheroids was initiated by plating cells ($5x10^3$/well) onto ultra low-adhesion round bottom 96-well plates followed by centrifugation at 1500 rpm for 10 min. The cross-sectional area was measured using phase contrast microscopy. Only H23 spheroids exhibited a typical spheroid morphology and measurable growth between day 3 and day 6 after plating.

First, the impact of 3-MP on H23 spheroid growth was assessed in conventional RPMI medium containing 11.1 mM glucose and 10% serum. When 3-MP was added 48 h after plating to H23 spheroids, the growth of the spheroids was significantly inhibited (Figure 18 *A*,*B*). This growth inhibition was concentration dependent (Figure 18 *B*). The growth inhibition by 3-MP in high glucose medium was caused by reduced proliferation, but not by the induction of apoptosis (Figure 18*C*).

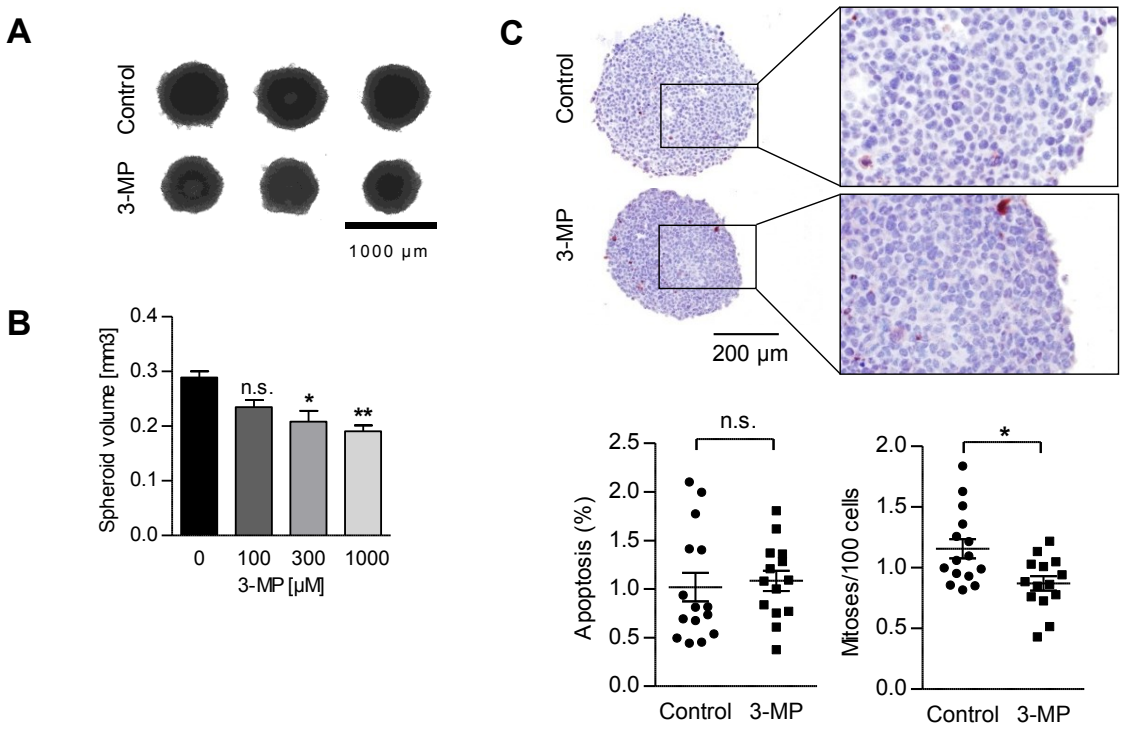

Figure 18. Impact of 3-mercaptopicolinate (3-MP) on spheroids in high glucose medium. Two days after the initiation of spheroid growth, 3-mercaptopicolinate (3-MP) was added to the culture medium. (**A**) Representative phase contrast images of spheroids treated with 1000 µM 3-MP or vehicle. Images were taken 10 days after plating. (**B**) The cross-sectional area was measured using phase contrast microscopy 10 days after plating. The volume *V* of the spheres was calculated from the cross-sectional radius. Results are mean +/- SEM from four independent experiments. (**C**) Spheroids were treated with 1000 µM 3-MP or vehicle. Five days after plating (three days after treatment) spheroids were fixed and paraffin-embedded. Serial sections of paraffin-embedded spheroids were stained with cleaved caspase 3 antibodies and counterstained with hematoxylin. Representative images are shown, with very few apoptotic cells in treated and un-treated spheroids. Lines indicate mean +/- SEM from all spheroids examined. * $P<0.05$, ** $P<0.01$.

An even more pronounced inhibition of spheroid growth by 3-MP was observed in medium containing a physiological glucose concentration (5 mM) (Figure 19). In the physiological glucose medium 3-MP led to significantly enhanced apoptosis and reduced proliferation (Figure 19). The difference in apoptosis was also significant if two 3-MP treated spheroids with very high apoptosis (14.5 and 15%), which represented outliers, were included in the analysis.

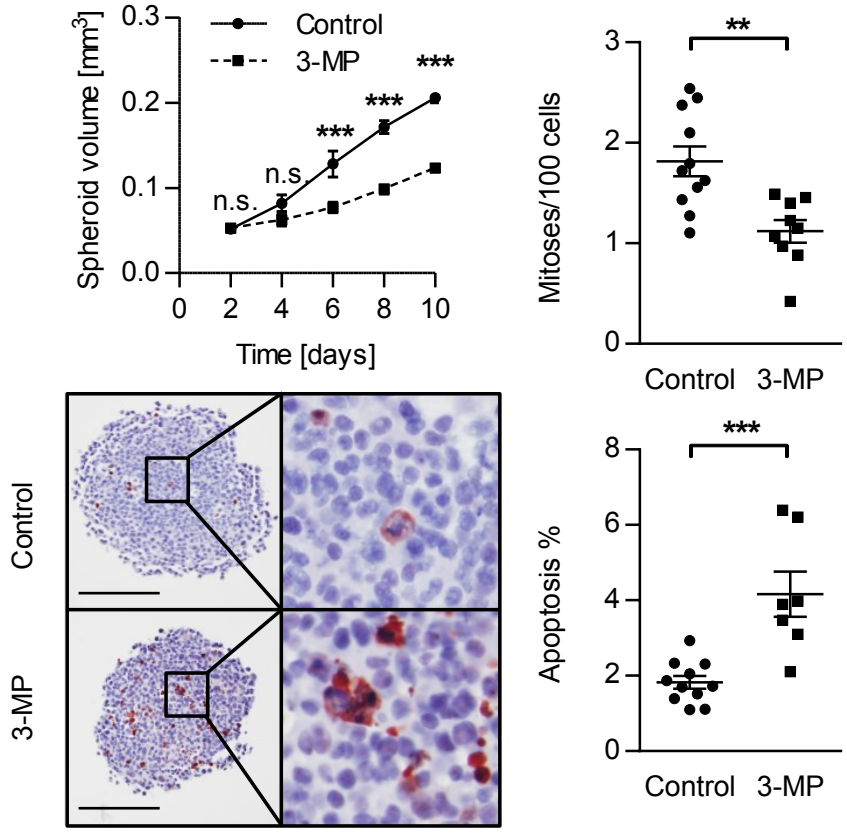

Figure 19. Impact of 3-mercaptopicolinate (3-MP) on spheroids in medium containing a physiological concentration glucose. Aggregation of H23 cells into spheroids was initiated by plating cells onto ultra low-adhesion round bottom 96-well plates in growth medium containing a physiological glucose concentration (5 mM), 10% dialyzed FBS and antibiotics. Two days after plating, 3-MP (1 mM) was added to the culture medium. The cross-sectional area was measured using phase contrast microscopy every second day after plating. Results are mean +/- SEM from three independent experiments. Five days after plating (three days after treatment) spheroids were fixed and paraffin-embedded. Serial sections were stained with cleaved caspase 3 antibodies and counterstained with hematoxylin. Representative sections are shown. The number of apoptoses, mitotic figures, and total cell numbers were determined. Lines indicate mean +/- SEM from all spheroids examined. Group comparisons were performed with Student´s t-test. Scale bar: 200µm.

8. Discussion

Tumor cells possess the ability to adapt to low glucose conditions (Izuishi et al., 2000) but the mechanisms are largely unknown. Our study is the first to examine in detail the expression and the activity of the key gluconeogenic enzyme PEPCK in non-hepatic cancers and to determine its role in the survival of cancer cells under glucose deprivation. Moreover we analyzed whether lactate may serve as a gluconeogenic precursor in cancer cells.

8.1. Lactate transport in cancer cells

In human lung cancers, lactate concentrations of 10 to 30 µmol/g dry weight have been measured (Fan et al., 2009; Kami et al., 2013), which equals to approximately 2.5 to 7.5 mM, if a wet to dry weight ratio of 4 is assumed (Thomlinson and Gray, 1955). This corresponds to the levels detected in experimental tumors (Walenta et al., 2001). Until recently it was not clear, whether lactate is solely produced by cancer cells, or whether lactate is also transported into cancer cells under certain conditions. In 2008 a group from Louvain (Belgium) observed lactate uptake under glucose shortage in SiHa cervix squamous cell carcinoma cancer cells (Sonveaux et al., 2008). The same was observed in P53-/- HCT116 colon carcinoma cells (Boidot et al., 2012). However, the metabolic fate of lactate in cancer cells remained unclear. In line with these data we observed a net consumption of lactate by NSCLC cells grown in low glucose, but not in high glucose.

The expression of lactate transporters has been studied in different cancers. In lung cancer, expression of MCT1, which mediates both, import and export of lactate, has been described (Koukourakis et al., 2007; Lee et al., 2011; Pinheiro et al., 2010) along with expression of MCT4 (Koukourakis et al., 2007; Pinheiro et al., 2010), which preferentially mediates lactate export . However there are conflicting results on the expression of MCT1 and MCT4 in the normal lung (Koukourakis et al., 2007; Pinheiro et al., 2010). In line with these data, our study shows both, MCT1 and MCT4 expression in NSCLC.

8.2. Previous reports on PEPCK in cancer

Only sparse data on PEPCK expression in cancers exist so far. Gauthier et al. (Gauthier et al., 1989) reported in 1989 on the activities of different enzymes in HT29 colon adenocarcinoma cells and found a PEPCK activity of 6.6 mU/mg protein when glucose was present and 17.1 mU/mg when glucose was absent. However, this issue was not followed up. In a study by Amuthan et al. (Amuthan et al., 2002) it was described that PEPCK activity was increased in A549 cells depleted of mitochondrial DNA (Amuthan et al., 2002). The authors provide no data on expression levels. In a study by Chun et al. (Chun et al., 2010) PCK2 mRNA was found to be up-regulated along with other glycerol-synthesis enzymes in colon cancer cells expressing oncogenic Kras and hypoxia-inducible factor (HIF) as well as in colon cancer samples compared to normal mucosa. Kung et al. (Kung et al., 2012) reported increased PCK2 levels, detected by expression microarrays, in A549 cells treated with an activator of PKM2, the M2 isoform of pyruvate kinase.

8.3. Glucose dependent expression of PCK2 in lung cancer

We found PCK2 expression in three NSCLC cell lines, and in most NSCLC samples. PCK2 expression peaked at a low glucose concentration (1 mM D-glucose, app one fifth of the normal blood glucose concentration). Results from experimental tumors suggest that the glucose concentration may decline almost to zero in central viable tumor areas (Schroeder et al., 2005; Walenta et al., 2001). Thus, the high PCK2 expression under 1 mM glucose appears to be relevant in lung cancers *in vivo*. PCK2 expression was not further enhanced at concentrations lower than 1 mM, but was even slightly decreased. This may be attributable to an energy crisis and ATP loss, since gluconeogenesis requires energy, as does activation of apoptosis.

8.4. PEPCK activity in lung cancer

In order to analyze whether PCK2 is active in NSCLC cells, an established PEPCK assay (Stark et al., 2009) was used. In this assay OAA produced by PEPCK is immediately reduced to malate in a coupled assay with malate dehydrogenase. The consumption rate of NADH is measured. As a positive control we used starved mouse liver lysates. We assessed PEPCK activity in NSCLC cells cultured in serum-depleted medium containing different glucose concentrations and 10 mM lactate as a gluconeogenic precursor. After low glucose, high lactate treatment, A549 and H23 cells showed mean PEPCK activities of app. 4 mU/mg protein, which corresponded to 30% of starved mouse liver lysates. In H1299 cells the PEPCK activity was lower. Mouse liver PEPCK activities were in the range of values reported in the literature (She et al., 2000).

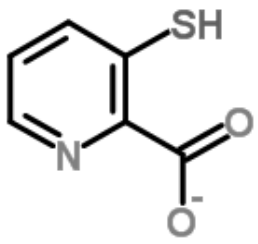

Figure 20. Structure of 3-mercaptopicolinate (3-MP), a reversible, non-competitive inhibitor or PCK1 and PCK2.

3-MP (Figure 20) is a reversible non-competitive inhibitor of PCK1 and PCK2 (Makinen and Nowak, 1983). Incubation of lysates (mouse liver or NSCLC cells) with 3-MP (1 mM) significantly reduced PEPCK activity, indicating that the assay specifically measured PEPCK activity. The concentration of 3-MP used in this study (up to 1 mM) is in the range of concentrations used in other studies.

In order to confirm the contribution of the PCK2 isoform to the measured PEPCK activities in NSCLC cell lines we used a commercially available PCK2 shRNA. We generated sub-populations of all three cell lines stably expressing PCK2 shRNA together with puromycin resistance gene, which served as a selection marker. For activity analyses this approach was preferred over siRNA due to the large amount

of cells needed in the experiments. A sufficient knockdown (at least 70% reduction on the mRNA level) was achieved only in A549, and H1299 cells, therefore these two cell lines were used for further shRNA experiments. We found that PEPCK activity was significantly lower in cells stably expressing PCK2 shRNA (Psh) in comparison to cells expressing a non-silencing shRNA (Csh). This further suggested that the PEPCK assay is specific. Moreover these data are in line with mRNA expression data showing that PCK2, but not PCK1, is expressed in NSCLC cells.

Importantly PEPCK activity was detectable in NSCLC samples obtained from surgery. PEPCK activity in tumors was significantly higher than PEPCK activity in corresponding normal lung tissue, which corresponds to PCK2 mRNA expression levels. This indicates that the PEPCK pathway is activated in human lung cancers *in vivo*.

8.5. Proof of the gluconeogenic pathway using stable isotope labelled lactate

PCK2 is generally regarded to mediate gluconeogenesis from lactate, since lactate conversion to pyruvate provides cytosolic NADH which is then available for the triosephosphate dehydrogenase reaction in gluconeogenesis (Watford et al., 1981). Stable isotope analysis was used to assess whether a metabolic flux from lactate to PEP via PEPCK occurs in NSCLC cells. Cells were allowed to adapt to low glucose high lactate conditions (1 mM D-glucose and 10 mM L-lactate in serum depleted medium) for 60 h. Thereafter lactate was replaced by $^{13}C_3$-lactate and cells were grown for additional 12 h. This medium replacement slightly reduced PEPCK activities in A549 cells as measured by the enzymatic assay. $^{13}C_3$-PEP was detectable in all NSCLC cell lines treated with $^{13}C_3$-lactate, whereas only small background signals were detectable in cells treated with unlabelled lactate, indicating that the conversion of $^{13}C_3$-lactate along the gluconeogenesis pathway occurred. In the presence of the PEPCK inhibitor 3-MP the ratio of labelled PEP to unlabelled PEP was significantly reduced, showing that the enrichment for $^{13}C_3$ in the PEP pool specifically occurred due to PEPCK.

In order to analyze the contribution of the PCK2 isoform to the measured PEPCK activities in NSCLC cell lines, we used A549 cells stably expressing PCK2 shRNA. We could not observe a reduction in $^{13}C_3$-PEP accumulation, however, the maximal reduction of PEPCK activity in A549 cells was only 37%. Metabolite levels are controlled by multiple enzymes, and a mild reduction of the activity or expression of an enzyme does not necessarily lead to altered levels of related metabolites (Fell, 2005).

Overall, the stable isotope experiments confirm that PCK2 metabolizes OAA in the direction of PEP in NSCLC cells under glucose depletion. All three carbons from $^{13}C_3$-lactate appeared in the PEP pool, thus confirming a direct conversion of lactate to PEP via PC. The rather low enrichment observed in our study might be attributable to dilution by PEP generated from other sources (from amino acids via PCK2, or from concomitant glycolysis).

8.6. Intracellular pathways regulating PCK2 expression and activity

While an array of publications exist on the regulation of PCK1 expression, only little is known about PCK2. This is maybe mainly related to the fact, that in the liver of mice, frequently used as model species, the majority of PEPCK activity is cytoplasmic. In contrast, in humans 50% of the liver PEPCK activity is mitochondrial (caused by PCK2), and 50% is cytoplasmic (caused by PCK1). However, the “strange case of PEPCK-M [PCK2]” increasingly draws attention (Yang et al., 2009a).

PCK1 activity is largely regulated on the transcriptional level (Yang et al., 2009b) (Figure 22). Since PEPCK plays a central role in glucose homeostasis in the body, the best characterized regulators of PCK1 are insulin, glucagon and glucocorticoids. During starvation, glucagon enhances expression of PCK1 via protein kinase A mediated phosphorylation of cAMP response element binding (CREB) and a parallel activation of CREB regulated transcriptional coactivator 2 (CRTC2) (Tsai et al., 2013). Moreover, glucagon activates CITED2 (CBP- and p300-interacting transactivator with glutamic acid– and aspartic acid–rich COOH-

terminal domain 2), a transcriptional co-regulator that interacts with numerous transcription factors (Sakai et al., 2012). Besides CREB other transcription factors are important for the activation of PEPCK (PCK1) transcription, namely hepatocyte nuclear factor 4α (HNF4α), the forkhead family member FOXO1, and peroxisome proliferator–activated receptor γ coactivator 1 (PGC-1α) (Herzig et al., 2001; Puigserver et al., 2003; Yoon et al., 2001). CREB either directly promotes PEPCK transcription, or via transcriptional up-regulation of PGC-1α (Herzig et al., 2001) (Figure 22). Interestingly, constitutive CREB activation plays an important role in cancer progression (for review see (Siu and Jin, 2007)).

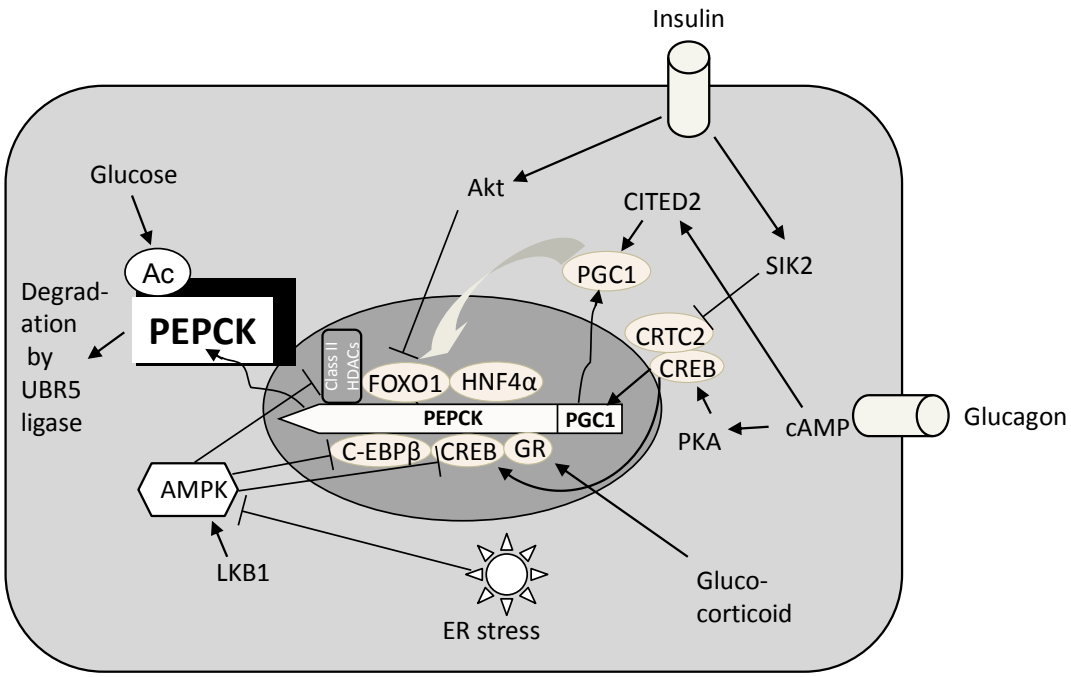

Figure 22. Intracellular signalling pathways leading to PEPCK expression. An explanation is given in the main text. Modified after (Oiso et al., 2011) and (Mihaylova and Shaw, 2013).

In addition to insulin and glucagon, non-hormonal signals are known to regulate gluconeogenesis. ER stress (endoplasmic reticulum stress), for example, enhances gluconeogenesis by inhibiting AMP-activated protein kinase (AMPK), which in turn leads to activation of C/EBPβ (Choudhury et al., 2011). AMPK is a central cellular energy sensor coordinating anabolic and catabolic pathways.

Specifically, AMPK limits energy consuming anabolic processes, like gluconeogenesis, and facilitates catabolic pathways (Viollet et al., 2009). AMPK is regulated by allosteric activators and phosphorylation (Viollet et al., 2009). It is activated by an increase in the AMP:ATP (adenosine monophosphate : adenosine triphosphate) ratio, either by increased ATP consumption or reduced ATP production following hypoxia, glucose deprivation, or inhibition of the mitochondrial respiratory chain. However, the activation of AMPK requires phosphorylation on Thr-172, which is accomplished by one of the three up-stream kinases, liver kinase B1 (LKB1), Ca^{2+}/calmodulin-dependent protein kinase kinase b (CaMKKb), and transforming growth factor (TGF)-β-activated kinase-1 (TAK1) (Viollet et al., 2009). The LKB1/AMPK pathway is an important negative regulator of gluconeogenesis in the liver (Viollet et al., 2009).

Glucose depletion may activate AMPK due to a decreased ATP production, which consequently limits gluconeogenesis, an ATP consuming process (Viollet et al., 2009). On the contrary, glucose depletion has been shown to activate gluconeogenesis by a reduction in PCK1 acetylation (Zhao et al., 2010), while high glucose led to PCK1 acetylation on Lys-70, Lys-71, and Lys-594, which in turn promoted PCK1 degradation (Zhao et al., 2010). Degradation of acetylated PCK1 was shown to be accomplished by the UBR5 ubiquitin ligase (Jiang et al., 2011) (Figure 22). The activation of PCK1 transcription has been shown to be controlled by histone deacetylases (HDACs) on different levels (Mihaylova and Shaw, 2013).

In contrast to PCK1, the regulation of the mitochondrial isoform of PEPCK (PCK2) is unclear. The PCK2 gene is located on chromosome 14q11.2-q12 in humans, in contrast to PCK1 which maps to 20q13.2-q13.31 (Yang et al., 2009a). Promoter analysis revealed that the PCK2 promoter harbours putative binding sites for transcription factors controlling also PCK1 expression (Table 4). Thus there is a potential overlap in signalling pathways controlling PCK1 and PCK2 expression, respectively. Interestingly PCK2 expression has been reported to be activated by the tumor suppressor p53 in HepG2 liver adenoma cells (Goldstein et al., 2013). In our study, however, the highest PEPCK activity was found in H23 cells, which have mutant p53 (Table 5). This argues against a major role of p53 in PCK2 activation in lung cancer cells. The mechanisms leading to PEPCK activation in

NSCLC cells under glucose depletion are at present unkown and need to be clarified in future studies.

Table 4. Putative binding sites in the PCK2 promoter

GR-alpha	NFI/CTF	NF-1	Elk-1	YY1	**HNF-4alpha**
AP-2alphaA	ETF	E2F	MAZ	TFIID	LEF-1
NF-AT1	c-Myb	STAT4	RXR-alpha	NF-AT2	TCF-4
GR-beta	ENKTF-1	TCF-4E	RAR-beta	STAT1beta	PR B
Pax-5	Sp1	ER-alpha	SRY	c-Jun	PR A
p53	TFII-I	c-Ets-2	**GR**	C/EBPalpha	EBF
XBP-1	c-Ets-1	IRF-1	E2F-1	NF-Y	
FOXP3	**C/EBPbeta**	WT1	GCF	PEA3	

Results from promoter analysis performed with the PROMO software (http://alggen.lsi.upc.es/cgi-bin/promo_v3/promo/promoinit.cgi?dirDB=TF_8.3). Transcription factors known to be important for PCK1 regulation are printed bold.

8.7. Potential role of LKB1 for activation of PCK2 in lung cancer cells

LKB1, also known as serine-threonine kinase 11 (STK11), was originally identified as the tumor suppressor gene responsible for the inherited cancer disorder Peutz-Jeghers-syndrome and is mutated in several types of cancer, e.g. in lung cancer (30% of patients) (Shackelford and Shaw, 2009). In our study we found that A549 and H23 cells, which lack functional LKB1 (Table 5) showed highest PEPCK activity, while H1299 had lowest enzyme activity, and lowest conversion to PEP. Furthermore, in A549 and H23 cells, but not in H1299 cells, glucose depletion-induced apoptosis was enhanced by PCK2 knockdown. The differences between H1299 and A549/H23 cells in respect to PCK2 activation and its function as “salvage pathway” may be attributable to their different LKB1 status. An increased capacity for glucose uptake in H1299 cells, or a reduced dependency on certain metabolites for survival, may also play a role. The high lactate consumption observed in H1299 cells appears to be primarily caused by conversion to acetyl CoA for ATP generation or fatty acid synthesis. Similar to the range of PEPCK activity found in lung cancer cell lines, a broad range in PCK2 expression and activity was found in NSCLC samples. The reason is at present unknown. To analyze the impact of mutations of LKB1, a likely candidate for PCK2 activation, would be highly interesting, however, our cohort was too small, to find possible

associations. Moreover the specific tumor region, perfusion, glucose availability, etc are expected to have considerable influence on PCK2 expression/activity, as is shown by our data, which further suggests the need for a higher patient number. We planned to analyze the role of LKB1 in a separate study.

Table 5. Genetic alterations in NSCLC cell lines

Cell line	*LKB1 (STK11)*	*KRAS*	*TP53*
A549	mt	mt	wt
H23	mt	mt	mt
H1299	wt	wt[a]	wt

Mutational data for *LKB1* were reported in (Sanchez-Cespedes et al., 2002); mutational data for *KRAS and TP53* genes were obtained from the Sanger Institute (COSMIC Cell Lines database; http://cancer.sanger.ac.uk/cancergenome/projects/cell_lines) and from (Sanchez-Cespedes et al., 2002) ; mt, inactivating mutation; wt, wild-type; [a] mutation in *NRAS*

8.8. PCK2 activation as salvage pathway under glucose depletion

NSCLC cells readily adapted to 1 mM glucose, however, severe glucose depletion (0.2 mM) led to the induction of cell death. Thus, we used medium containing 0.2 mM glucose to analyze the impact of PCK2 on cell survival. Transfection with PCK2 siRNA reduced PCK2 expression. PCK2 siRNA and treatment with 3-MP led to a significant increase in glucose depletion-induced apoptosis in A549 and H23 cells, while in H1299 no significant effect was found. Under high glucose conditions PCK2 siRNA had no effect. When necrosis/late apoptosis was assessed using a propidium iodide exclusion assay, a similar but less pronounced increase was found with PCK2 siRNA under low glucose, indicating that PCK2 primarily protects from apoptosis. As control siRNA, a pool of siRNA sequences proven not to affect any known gene was used. The control siRNA transfected cells were observed to resemble non-transfected cells in apoptosis sensitivity.

We generated sub-populations of all three cell lines stably expressing commercially available PCK2 shRNA. The knockdown-effects were highly variable in the three different cell lines. In H1299 cells a knockdown of more than 70% (on the mRNA level) was readily achieved, while in A549 cells the maximal knockdown was 65%, which corresponded to an even smaller decrease in PEPCK activity (37% decrease), maybe due to posttranslational effects. Puromycin selection as such obviously led to enhanced apoptosis resistance in A549 cells transfected with non-silencing shRNA, with only very sparse floating cells under glucose depletion in phase contrast microscopy and an average rate of apoptosis of only 7.7%. In H23 cells only a very mild knockdown was achieved with one out of four constructs, the maximal knockdown on the mRNA level was 33% and on the activity level 17%. Thus, unfortunately, the effects of PCK2 knockdown on apoptosis could not be assessed using shRNA. Still, we could demonstrate that different strategies to reduce PCK2 (siRNA pool and PEPCK inhibitor) led to the same effects on apoptosis.

8.9. Role of PCK2 in spheroid growth

Multicellular spheroids serve as a 3D cancer model which mimics the metabolic microenvironment of cancers in vivo, since inside such spheroids gradients for nutrients and oxygen occur (Dang and Semenza, 1999; Hirschhaeuser et al., 2010) (Figure 23).

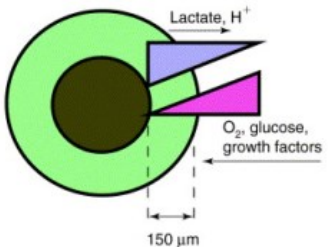

Figure 23. Properties of multicellular spheroids. On the surface oxygen and glucose concentrations are determined by the surrounding growth medium. Inside the spheroids gradients occur due to consumption and limited diffusion. On the other hand the concentrations of lactate and H^+, which are released by the tumor cells as a consequence of enhanced glycolysis (Warburg effect), are highest close to the center of the spheroid, while lactate and H^+ easily diffuse into the medium from the outer layers. The dark circle in

the middle represents the necrotic center frequently found in larger spheroids from different cells lines. Figure from (Dang and Semenza, 1999).

All three cell lines were screened for the ability to grow as spheroids. All three cell lines had a typical spheroid morphology 48 h after plating and centrifugation in the ultra-low adhesion cell culture 96-well plates, however, only one cell line (H23) showed an increase in spheroid size. Such limited spheroid forming capabilities of cancer cell lines are frequently observed (A.L. Harris, Weatherall Institute of Molecular Medicine, University of Oxford, personal communication).

When 3-MP was added 48 h after plating to H23 spheroids cultured in conventional RPMI medium containing 11.1 mM glucose and 10% FBS, growth of the spheroids was significantly inhibited. This growth inhibition was concentration dependent. An even more pronounced inhibition of spheroid growth by 3-MP was observed in medium containing a physiological glucose concentration of 5 mM supplemented with 10% dialyzed FBS. In the physiological glucose environment 3-MP led to significantly enhanced apoptosis and reduced proliferation. In contrast, in high glucose medium 3-MP influenced proliferation but did not cause apoptosis. These results suggest that PEPCK inhibition causes an increase in cancer cell apoptosis in the microenvironment in spheroids, which mimics the microenvironment present in cancers *in vivo*.

8.10. Proposed novel metabolic pathway in cancer cells involving PC and PCK2

We found that the mitochondrial isoform of PEPCK, PCK2 rather than PCK1 was expressed in NSCLC cell lines and in NSCLC tissue. PCK2 is generally regarded to mediate gluconeogenesis from lactate, since lactate conversion to pyruvate provides cytosolic NADH which is then available for the triosephosphate dehydrogenase reaction in gluconeogenesis (Watford et al., 1981). In fact, we observed a conversion of $^{13}C_3$-lactate to $^{13}C_3$-PEP in NSCLC cells, thus confirming that lactate is a gluconeogenic precursor in lung cancer cells. All three carbons from $^{13}C_3$-lactate appeared in the PEP pool, thus confirming a direct conversion of lactate to pyruvate, pyruvate to OAA and OAA to PEP in cancer cells (Figure 21).

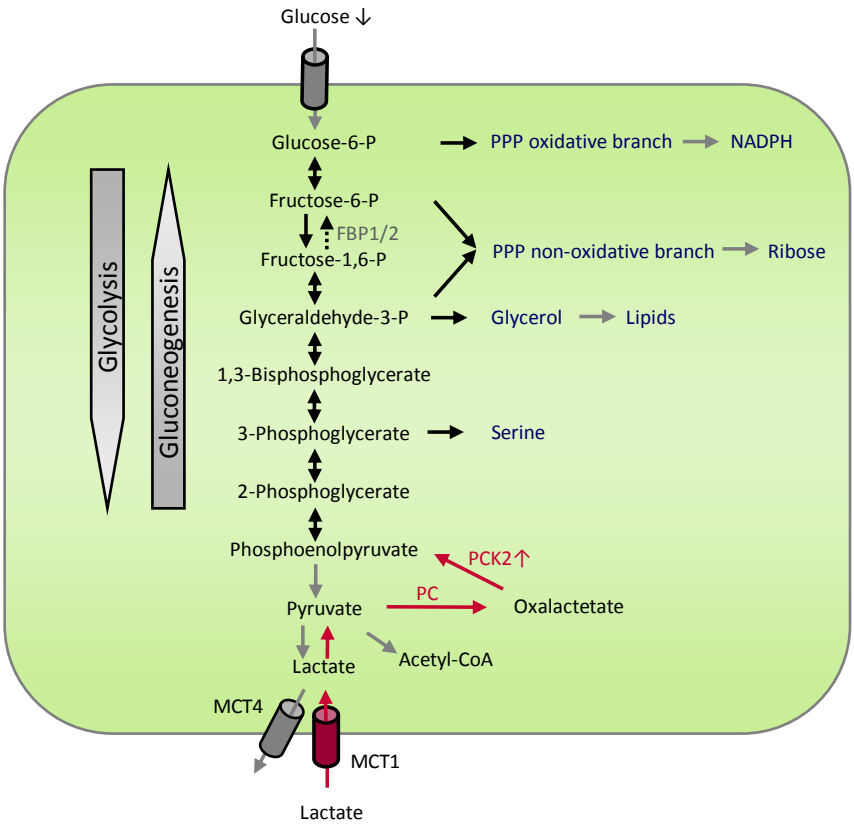

Figure 21. Proposed metabolic pathway activated in cancer cells lacking glucose. Dotted arrows are glycolysis reactions, red arrows show gluconeogenesis, which is activated under glucose shortage. FBP1, fructose-1,6-biphosphatase; PPP, pentose phosphate pathway; PCK2, mitochondrial isoform of phosphoenolpyruvate carboxykinase; PC, pyruvate carboxylase; MCT1, monocarboxylate transporter 1; MCT4, monocarboxylate transporter 4.

Conversion of pyruvate to OAA requires PC. We show that PC is constitutively expressed in all three lung cancer cell lines analyzed. PC expression has been described previously to occur in cancers (Cheng et al., 2011; Fan et al., 2009). It has been suggested that PC helps to refill the TCA cycle (anaplerosis) by converting pyruvate to OAA (Cheng et al., 2011). The exact role of PC in cancer cells, either generation of OAA for anaplerosis, or generation of OAA for gluconeogenesis may depend on the metabolic requirements of the cell and the availability of nutrients.

With one exception all reactions in glycolysis upstream of PEP and downstream of glucose-6-phosphate are reversible (Stryer, 1995). Thus, PCK2, by its contribution to the PEP pool, could give rise to a number of biosynthetic processes even in the

absence of glucose, especially serine and glycerol synthesis (Kalhan and Hanson, 2012; Yang et al., 2009a). Potentially, PEP may be shuttled also to ribose generation required for nucleotide synthesis, via the non-oxidative PPP and might fuel the oxidative PPP resulting in NADPH generation. The latter two pathways would require another gluconeogenic enzyme, fructose-1,6-biphosphatase (FBP), which exists in two isoforms, FBP1 and FBP2 (Figure 21). FBP1 is inhibited by fructose-2,6-biphosphate (Okar et al., 2001), a metabolite that is degraded e.g. by the tumor promoting fructose-2,6-bisphosphatase TIGAR (Bensaad et al., 2006; Cheung et al., 2013). The role of FBP in cancer cells is unknown and should be analyzed in future studies.

8.11. Potential role of PCK2 in the anti-cancer effect of metformin

Metformin is a widely used biguanide for the treatment of type 2 diabetes. Metformin induces an increase in the intracellular AMP:ATP ratio, which in turn activates AMPK (Goodwin et al., 2009). AMPK activation by metformin, with a resulting decrease in the expression of gluconeogenic enzymes, is responsible for inhibition of liver gluconeogenesis (Rizos and Elisaf, 2013). Traditionally inhibition of complex I of the respiratory chain by metformin has been regarded as the underlying mechanism (Owen et al., 2000), however, this view was challenged by a recent publication showing that metformin increased mitochondrial respiration (Vytla and Ochs, 2013).

A few years ago it has been recognized in retrospective studies, that metformin reduced the risk to develop cancer (for review see (Rizos and Elisaf, 2013)). A direct effect of metformin on cancer cell growth has also been observed in numerous *in vitro* studies (Rizos and Elisaf, 2013). Unfortunately in many *in vitro* studies very high concentrations of metformin have been used (concentrations of up to 20 mM, while the therapeutic plasma level is 2.8–15 μM) (Rizos and Elisaf, 2013), which makes an interpretation of the results difficult. Nevertheless, there are at present more than 180 clinical trials on the way to assess possible beneficial effects of metformin in cancer patients (www.clinicaltrials.gov). The exact mechanism of metformin action on cancer cells is not known. Activation of

AMPK seems to play a major role (Goodwin et al., 2009). Interestingly, it has been found, that glucose deprivation sensitizes cancer cells to metformin (Menendez et al., 2012). At present it is not known, whether inhibition of PEPCK in cancer cells contributes to the anti-cancer effect of metformin. Further studies are warranted to answer this question.

8.12. Current concepts of cancer cell adaptation to the microenvironment

The six hallmark characteristics of cancer cells, defined in the highly cited work by D. Hanahan and R.A. Weinberg (Hanahan and Weinberg, 2000) in 2000, encompassed sustained proliferative signalling, resistance to growth suppressors, resistance to cell death, replicative immortality, induction of angiogenesis, and activation of invasion and metastasis. In their novel description of cancer "hallmarks" (Hanahan and Weinberg, 2011), D. Hanahan and R.A. Weinberg focussed on the constitution of the tumor microenvironment, in which cancer cells are embedded and which is in constant interaction with the neoplastic cancer cells. Hypoxia, nutrient depletion, and lactate accumulation are typically present in the microenvironment, especially in solid cancers (Cairns et al., 2011; Cantor and Sabatini, 2012; Romero-Garcia et al., 2011). The neoplastic tumor cells themselves shape the microenvironment in the multistep process of tumorigenesis (Hanahan and Weinberg, 2011) including angiogenesis.

In order to ensure the supply with oxygen and nutrients, cancer cells stimulate the growth of new blood vessels (angiogenesis), a phenomenon which has been described already 40 years ago (Folkman, 1971). Since vascular endothelial growth factor (VEGF) was identified as major angiogenic factor released by cancer cells, numerous clinical trials have been performed with different agents targeting VEGF or other angiogenic factors (Singh and Ferrara, 2012), leading to the approval of VEGF inhibitors (e.g. bevacizumab) for the treatment of several solid cancers, including lung cancer (Singh and Ferrara, 2012). However, the magnitude of the clinical benefit with anti-angiogenic drugs has been rather modest across several tumor types (Mountzios et al., 2014). VEGF-targeted treatment, despite being effective in reducing primary tumor growth initially, in fact

results in a more invasive, aggressive phenotype by aggravating intratumoral hypoxia (Carmeliet and Jain, 2011; Harris, 2002; Höckel and Vaupel, 2001; Mountzios et al., 2014; Semenza, 2010). This effect is related to the capability of cancer cells to adapt to changes in the microenvironment.

The adaptive changes evoked by hypoxia have been intensively studied in the past years. They involve the neoplastic cancer cells, but also the accompanying stroma cells (Giaccia and Schipani, 2010). In contrast to hypoxia, the effects of a reduction of glucose in the microenvironment, are poorly understood. One of the mechanisms recently described is up-regulation of glucose transporter GLUT1 (Guenther et al., 2013). Interestingly, enzymes responsible for amino acid synthesis and transport also seem to be affected by the extracellular glucose concentration. Both, amino acid and glucose deprivation have been shown to induce expression of the asparagine synthase, which catalyses the biosynthesis of asparagine from aspartate and glutamine (Barbosa-Tessmann et al., 1999). Amino acid and glucose deprivation have been shown to activate eukaryotic initiation factor 2α and thereby to up-regulate genes involved in amino acid synthesis and transport (Ye et al., 2010). Storage of glucose in the form of glycogen, which is activated by hypoxia, was shown to protect cancer cells from acute glucose deprivation (Pelletier et al., 2012).

Recently, colon cancer cells lacking glucose were shown by Ma et al. (Ma et al., 2013) to avidly consume glutamine, an effect that was enhanced by knockdown of protein kinase C zeta (PKCζ). Interestingly, carbon derived from uniformly ^{13}C-labelled glutamine was detected in 3-phopshoglycerate, an important precursor of serine, in serine, and in glycine in that study (Ma et al., 2013). In addition, PKCζ was shown to modulate expression of serine biosynthetic enzymes (Ma et al., 2013). Although these findings provide an indirect evidence for PEPCK action in these cells, PEPCK was not analyzed or mentioned in that study (Ma et al., 2013). However, the study by Ma et al. (Ma et al., 2013) provides additional evidence for the metabolic plasticity of cancer cells.

Due to the emerging understanding of cancer cell metabolism, D. Hanahan and R.A. Weinberg definded reprogramming energy metabolism as a novel cancer hallmark (Hanahan and Weinberg, 2011). Although it was discussed occasionally in the past years, that reprogramming of cancer metabolism and adaptation of cancer cells to the microenvironment occur at the same time and are interrelated (Cairns et al., 2011; Cantor and Sabatini, 2012; Romero-Garcia et al., 2011), the two cancer hallmarks are frequently viewed separately. By showing that cancer cells need to switch from predominant glycolysis to gluconeogenesis in response to reduced glucose concentration in the microenvironment, we provide evidence that metabolic autonomy and flexibility are important cancer cell strategies. These strategies may be important for cancer progression along with growth promoting metabolic reprogramming (the Warburg effect), and may limit cancer cell death in an unfavourable tumor microenvironment. The proposed metabolic network of glycolysis and gluconeogenesis, acting in concert to promote cancer growth, is depicted in Figure 24.

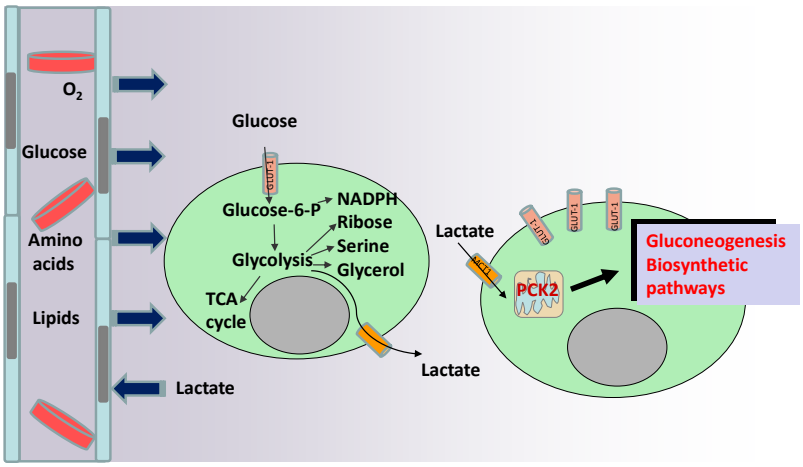

Figure 24. Proposed metabolic network in lung cancers. Glucose is metabolized by cancer cells primarily through glycolysis, in order to provide cellular building blocks and NADPH. In solid cancers the demand for glucose is not balanced by adequate supply. Thus glucose levels, similar to oxygen levels, decline with increasing distance from perfused capillaries (vessels). As shown in the present study, the mitochondrial gluconeogenic enzyme PCK2 is activated in lung cancer cells when glucose levels drop, which improves cell survival. Numerous biosynthetic pathways originate from the gluconeogenesis pathway, which is in many aspects the reverse of glycolysis, allowing the cells to compensate for glucose shortage. As shown in this study, lactate, which is present in huge amounts in solid cancers, is metabolized via this novel pathway.

Appreciation of the specific tumor microenvironment is an important task for future research on cancer metabolism. Metabolic flux studies using stable isotopes in cancer models *in vivo* will help to analyze the metabolism of cancer cells with a natural supply of nutrients and oxygen (Marin-Valencia et al., 2012). However, it is possible to simulate certain aspects of cancer microenvironment also *in vitro*, as was done in our study. The use of appropriate glucose concentrations in the media is crucial. Many culture media contain more than 10 mM glucose (often even 25 mM). In normal individuals the average plasma glucose concentration is approximately 5.5 mM (100 mg/dl), and glucose levels rarely exceed 7.8 mM (140 mg/dl) after meals (American Diabetes Association, 2001; Juvenile Diabetes Research Foundation Continuous Glucose Monitoring Study Group, 2010). In tumors much lower glucose levels are found (Hirayama et al., 2009; Rocha et al., 2010). Thus cell culture media often reflect (pre-) diabetic conditions rather than the low glucose environment found in tumors. The use of cell culture conditions mimicking the normal tumor microenvironment may help understanding tumor metabolism *in vivo*.

8.13. Conclusion

In summary the present study shows for the first time that the gluconeogenic key enzyme PCK2 is expressed and active in lung cancer cells and that lactate may serve as a gluconeogenic precursor in these cells. As a conclusion non-hepatic cancer cells may utilize at least some steps of gluconeogenesis in order to adapt to low glucose conditions. Further studies are warranted to analyze the mechanisms of PCK2 and the downstream metabolic pathways of PCK2.

9. Bibiography

American Diabetes Association. (2001). Postprandial blood glucose. American Diabetes Association. Diabetes Care *24,* 775-778.

Amuthan, G., Biswas, G., Ananadatheerthavarada, H.K., Vijayasarathy, C., Shephard, H.M., and Avadhani, N.G. (2002). Mitochondrial stress-induced calcium signaling, phenotypic changes and invasive behavior in human lung carcinoma A549 cells. Oncogene *21,* 7839-7849.

Barbosa-Tessmann, I.P., Pineda, V.L., Nick, H.S., Schuster, S.M., and Kilberg, M.S. (1999). Transcriptional regulation of the human asparagine synthetase gene by carbohydrate availability. Biochem. J. *339 (Pt 1),* 151-158.

Bensaad, K., Tsuruta, A., Selak, M.A., Vidal, M.N., Nakano, K., Bartrons, R., Gottlieb, E., and Vousden, K.H. (2006). TIGAR, a p53-inducible regulator of glycolysis and apoptosis. Cell *126,* 107-120.

Bensinger, S.J., and Christofk, H.R. (2012). New aspects of the Warburg effect in cancer cell biology. Semin. Cell Dev. Biol. *23,* 352-361.

Boidot, R., Vegran, F., Meulle, A., Le Breton, A., Dessy, C., Sonveaux, P., Lizard-Nacol, S., and Feron, O. (2012). Regulation of monocarboxylate transporter MCT1 expression by p53 mediates inward and outward lactate fluxes in tumors. Cancer Res. *72,* 939-948.

Cagle, P.T. (2010). Epidemiology and demographics of lung cancer. In Advances in Surgical Pathology: Lung Cancer, Cagle, P. T., and Allen, T. eds., (Philadelphia: Wolters Kluwer Health)

Cairns, R.A., Harris, I.S., and Mak, T.W. (2011). Regulation of cancer cell metabolism. Nat. Rev. Cancer. *11,* 85-95.

Cantor, J.R., and Sabatini, D.M. (2012). Cancer cell metabolism: one hallmark, many faces. Cancer. Discov. *2,* 881-898.

Carmeliet, P., and Jain, R.K. (2011). Molecular mechanisms and clinical applications of angiogenesis. Nature *473,* 298-307.

Cheng, T., Sudderth, J., Yang, C., Mullen, A.R., Jin, E.S., Mates, J.M., and DeBerardinis, R.J. (2011). Pyruvate carboxylase is required for glutamine-independent growth of tumor cells. Proc. Natl. Acad. Sci. U. S. A. *108,* 8674-8679.

Cheung, E.C., Athineos, D., Lee, P., Ridgway, R.A., Lambie, W., Nixon, C., Strathdee, D., Blyth, K., Sansom, O.J., and Vousden, K.H. (2013). TIGAR Is Required for Efficient Intestinal Regeneration and Tumorigenesis. Dev. Cell. *25,* 463-477.

Choudhury, M., Qadri, I., Rahman, S.M., Schroeder-Gloeckler, J., Janssen, R.C., and Friedman, J.E. (2011). C/EBPbeta is AMP kinase sensitive and up-regulates PEPCK in response to ER stress in hepatoma cells. Mol. Cell. Endocrinol. *331,* 102-108.

Christofk, H.R., Vander Heiden, M.G., Harris, M.H., Ramanathan, A., Gerszten, R.E., Wei, R., Fleming, M.D., Schreiber, S.L., and Cantley, L.C. (2008). The M2 splice isoform of pyruvate kinase is important for cancer metabolism and tumour growth. Nature *452,* 230-233.

Chun, S.Y., Johnson, C., Washburn, J.G., Cruz-Correa, M.R., Dang, D.T., and Dang, L.H. (2010). Oncogenic KRAS modulates mitochondrial metabolism in human colon cancer cells by inducing HIF-1alpha and HIF-2alpha target genes. Mol. Cancer. *9,* 293-4598-9-293.

Dang, C.V., and Semenza, G.L. (1999). Oncogenic alterations of metabolism. Trends Biochem. Sci. *24,* 68-72.

DeBerardinis, R.J., and Thompson, C.B. (2012). Cellular metabolism and disease:

what do metabolic outliers teach us? Cell *148,* 1132-1144.

Ding, L., Getz, G., Wheeler, D.A., Mardis, E.R., McLellan, M.D., Cibulskis, K., Sougnez, C., Greulich, H., Muzny, D.M., Morgan, M.B., *et al.* (2008). Somatic mutations affect key pathways in lung adenocarcinoma. Nature *455,* 1069-1075.

Engle, M.J., Dooley, M., and Brown, D.J. (1987). Evidence for lactate utilization for fetal lung glycogen synthesis. Biochem. Biophys. Res. Commun. *145,* 397-401.

Fan, T.W., Lane, A.N., Higashi, R.M., Farag, M.A., Gao, H., Bousamra, M., and Miller, D.M. (2009). Altered regulation of metabolic pathways in human lung cancer discerned by (13)C stable isotope-resolved metabolomics (SIRM). Mol. Cancer *8,* 41.

Fell, D.A. (2005). Enzymes, metabolites and fluxes. J. Exp. Bot. *56,* 267-272.
Folkman, J. (1971). Tumor angiogenesis: therapeutic implications. N. Engl. J. Med. *285,* 1182-1186.

Gauthier, T., Denis-Pouxviel, C., and Murat, J.C. (1989). Carbohydrate metabolism in HT29 colon cancer cells cultured in a glucose free medium supplemented with inosine. Int. J. Biochem. *21,* 191-196.

Giaccia, A.J., and Schipani, E. (2010). Role of carcinoma-associated fibroblasts and hypoxia in tumor progression. Curr. Top. Microbiol. Immunol. *345,* 31-45.

Goldstein, I., Yizhak, K., Madar, S., Goldfinger, N., Ruppin, E., and Rotter, V. (2013). P53 Promotes the Expression of Gluconeogenesis-Related Genes and Enhances Hepatic Glucose Production. Cancer. Metab. *1,* 9-3002-1-9.

Goodwin, P.J., Ligibel, J.A., and Stambolic, V. (2009). Metformin in breast cancer: time for action. J. Clin. Oncol. *27,* 3271-3273.

Guenther, G.G., Liu, G., Ramirez, M.U., McMonigle, R.J., Kim, S.M., McCracken, A.N., Joo, Y., Ushach, I., Nguyen, N.L., and Edinger, A.L. (2013). Loss of TSC2

confers resistance to ceramide and nutrient deprivation. Oncogene

Halestrap, A.P. (2012). The monocarboxylate transporter family--Structure and functional characterization. IUBMB Life *64,* 1-9.

Hanahan, D., and Weinberg, R.A. (2011). Hallmarks of cancer: the next generation. Cell *144,* 646-674.

Hanahan, D., and Weinberg, R.A. (2000). The hallmarks of cancer. Cell *100,* 57-70.

Harris, A.L. (2002). Hypoxia - a key regulatory factor in tumour growth. Nat. Rev. Cancer *2,* 38-47.

Heist, R.S., Sequist, L.V., and Engelman, J.A. (2012). Genetic changes in squamous cell lung cancer: a review. J. Thorac. Oncol. *7,* 924-933.

Herzig, S., Long, F., Jhala, U.S., Hedrick, S., Quinn, R., Bauer, A., Rudolph, D., Schutz, G., Yoon, C., Puigserver, P., Spiegelman, B., and Montminy, M. (2001). CREB regulates hepatic gluconeogenesis through the coactivator PGC-1. Nature *413,* 179-183.

Hirayama, A., Kami, K., Sugimoto, M., Sugawara, M., Toki, N., Onozuka, H., Kinoshita, T., Saito, N., Ochiai, A., Tomita, M., Esumi, H., and Soga, T. (2009). Quantitative metabolome profiling of colon and stomach cancer microenvironment by capillary electrophoresis time-of-flight mass spectrometry. Cancer Res. *69,* 4918-4925.

Hirschhaeuser, F., Menne, H., Dittfeld, C., West, J., Mueller-Klieser, W., and Kunz-Schughart, L.A. (2010). Multicellular tumor spheroids: an underestimated tool is catching up again. J. Biotechnol. *148,* 3-15.

Höckel, M., and Vaupel, P. (2001). Tumor hypoxia: definitions and current clinical, biologic, and molecular aspects. J. Natl. Cancer Inst. *93,* 266-276.

Izuishi, K., Kato, K., Ogura, T., Kinoshita, T., and Esumi, H. (2000). Remarkable tolerance of tumor cells to nutrient deprivation: possible new biochemical target for cancer therapy. Cancer Res. *60,* 6201-6207.

Jiang, W., Wang, S., Xiao, M., Lin, Y., Zhou, L., Lei, Q., Xiong, Y., Guan, K.L., and Zhao, S. (2011). Acetylation regulates gluconeogenesis by promoting PEPCK1 degradation via recruiting the UBR5 ubiquitin ligase. Mol. Cell *43,* 33-44.

Juvenile Diabetes Research Foundation Continuous Glucose Monitoring Study Group, Fox, L.A., Beck, R.W., and Xing, D. (2010). Variation of interstitial glucose measurements assessed by continuous glucose monitors in healthy, nondiabetic individuals. Diabetes Care *33,* 1297-1299.

Kalhan, S.C., and Hanson, R.W. (2012). Resurgence of serine: an often neglected but indispensable amino Acid. J. Biol. Chem. *287,* 19786-19791.

Kami, K., Fujimori, T., Sato, H., Sato, M., Yamamoto, H., Ohashi, Y., Sugiyama, N., Ishihama, Y., Onozuka, H., Ochiai, A.*, et al.* (2013). Metabolomic profiling of lung and prostate tumor tissues by capillary electrophoresis time-of-flight mass spectrometry. Metabolomics *9,* 444-453.

Koppenol, W.H., Bounds, P.L., and Dang, C.V. (2011). Otto Warburg's contributions to current concepts of cancer metabolism. Nat. Rev. Cancer. *11,* 325-337.

Kothmaier, H., Quehenberger, F., Halbwedl, I., Morbini, P., Demirag, F., Zeren, H., Comin, C.E., Murer, B., Cagle, P.T., Attanoos, R.*, et al.* (2008). EGFR and PDGFR differentially promote growth in malignant epithelioid mesothelioma of short and long term survivors. Thorax *63,* 345-351.

Koukourakis, M.I., Giatromanolaki, A., Bougioukas, G., and Sivridis, E. (2007). Lung cancer: a comparative study of metabolism related protein expression in cancer cells and tumor associated stroma. Cancer. Biol. Ther. *6,* 1476-1479.

Kung, C., Hixon, J., Choe, S., Marks, K., Gross, S., Murphy, E., DeLaBarre, B., Cianchetta, G., Sethumadhavan, S., Wang, X.*, et al.* (2012). Small molecule activation of PKM2 in cancer cells induces serine auxotrophy. Chem. Biol. *19,* 1187-1198.

Landi, M.T., Dracheva, T., Rotunno, M., Figueroa, J.D., Liu, H., Dasgupta, A., Mann, F.E., Fukuoka, J., Hames, M., Bergen, A.W.*, et al.* (2008). Gene expression signature of cigarette smoking and its role in lung adenocarcinoma development and survival. PLoS One *3,* e1651.

Lee, G.H., Kim, D.S., Chung, M.J., Chae, S.W., Kim, H.R., and Chae, H.J. (2011). Lysyl oxidase-like-1 enhances lung metastasis when lactate accumulation and monocarboxylate transporter expression are involved. Oncol. Lett. *2,* 831-838.

Leithner, K., Wohlkoenig, C., Stacher, E., Lindenmann, J., Hofmann, N.A., Galle, B., Guelly, C., Quehenberger, F., Stiegler, P., Smolle-Juttner, F.M.*, et al.* (2014a). Hypoxia increases membrane metallo-endopeptidase expression in a novel lung cancer ex vivo model - role of tumor stroma cells. BMC Cancer *14,* 40.

Leithner, K., Hrzenjak, A., Trötzmüller, M., Moustafa, T., Köfeler, H.C., Wohlkoenig, C., Stacher, E., Lindenmann, J., Harris, A.L., Olschewski, A., and Olschewski, H. (2014b). PCK2 activation mediates an adaptive response to glucose depletion in lung cancer . Oncogene *2014* Mar 17. doi: 10.1038/onc.2014.47. [Epub ahead of print]

Ma, L., Tao, Y., Duran, A., Llado, V., Galvez, A., Barger, J.F., Castilla, E.A., Chen, J., Yajima, T., Porollo, A.*, et al.* (2013). Control of nutrient stress-induced metabolic reprogramming by PKCzeta in tumorigenesis. Cell *152,* 599-611.

Makinen, A.L., and Nowak, T. (1983). 3-Mercaptopicolinate. A reversible active site inhibitor of avian liver phosphoenolpyruvate carboxykinase. J. Biol. Chem. *258,* 11654-11662.

Marin-Valencia, I., Yang, C., Mashimo, T., Cho, S., Baek, H., Yang, X.L., Rajagopalan, K.N., Maddie, M., Vemireddy, V., Zhao, Z.*, et al.* (2012). Analysis of tumor metabolism reveals mitochondrial glucose oxidation in genetically diverse human glioblastomas in the mouse brain in vivo. Cell. Metab. *15,* 827-837.

Menendez, J.A., Oliveras-Ferraros, C., Cufi, S., Corominas-Faja, B., Joven, J., Martin-Castillo, B., and Vazquez-Martin, A. (2012). Metformin is synthetically lethal with glucose withdrawal in cancer cells. Cell. Cycle *11,* 2782-2792.

Mihaylova, M.M., and Shaw, R.J. (2013). Metabolic reprogramming by class I and II histone deacetylases. Trends Endocrinol. Metab. *24,* 48-57.

Mountzios, G., Pentheroudakis, G., and Carmeliet, P. (2014). Bevacizumab and micrometastases: Revisiting the preclinical and clinical rollercoaster. Pharmacol. Ther. *141,* 117-124.

Oiso, H., Furukawa, N., Suefuji, M., Shimoda, S., Ito, A., Furumai, R., Nakagawa, J., Yoshida, M., Nishino, N., and Araki, E. (2011). The role of class I histone deacetylase (HDAC) on gluconeogenesis in liver. Biochem. Biophys. Res. Commun. *404,* 166-172.

Okar, D.A., Manzano, A., Navarro-Sabate, A., Riera, L., Bartrons, R., and Lange, A.J. (2001). PFK-2/FBPase-2: maker and breaker of the essential biofactor fructose-2,6-bisphosphate. Trends Biochem. Sci. *26,* 30-35.

Owen, M.R., Doran, E., and Halestrap, A.P. (2000). Evidence that metformin exerts its anti-diabetic effects through inhibition of complex 1 of the mitochondrial respiratory chain. Biochem. J. *348 Pt 3,* 607-614.

Pelletier, J., Bellot, G., Gounon, P., Lacas-Gervais, S., Pouyssegur, J., and Mazure, N.M. (2012). Glycogen Synthesis is Induced in Hypoxia by the Hypoxia-Inducible Factor and Promotes Cancer Cell Survival. Front. Oncol. *2,* 18.

Pinheiro, C., Reis, R.M., Ricardo, S., Longatto-Filho, A., Schmitt, F., and Baltazar,

F. (2010). Expression of monocarboxylate transporters 1, 2, and 4 in human tumours and their association with CD147 and CD44. J. Biomed. Biotechnol. *2010,* 427694.

Polet, F., and Feron, O. (2013). Endothelial cell metabolism and tumour angiogenesis: glucose and glutamine as essential fuels and lactate as the driving force. J. Intern. Med. *273,* 156-165.

Puigserver, P., Rhee, J., Donovan, J., Walkey, C.J., Yoon, J.C., Oriente, F., Kitamura, Y., Altomonte, J., Dong, H., Accili, D., and Spiegelman, B.M. (2003). Insulin-regulated hepatic gluconeogenesis through FOXO1-PGC-1alpha interaction. Nature *423,* 550-555.

Ramalingam, S.S., Owonikoko, T.K., and Khuri, F.R. (2011). Lung cancer: New biological insights and recent therapeutic advances. CA Cancer. J. Clin. *61,* 91-112.

Reck, M., Heigener, D.F., Mok, T., Soria, J.C., and Rabe, K.F. (2013). Management of non-small-cell lung cancer: recent developments. Lancet *382,* 709-719.

Rizos, C.V., and Elisaf, M.S. (2013). Metformin and cancer. Eur. J. Pharmacol. *705,* 96-108.

Roberts, P.J., Stinchcombe, T.E., Der, C.J., and Socinski, M.A. (2010). Personalized medicine in non-small-cell lung cancer: is KRAS a useful marker in selecting patients for epidermal growth factor receptor-targeted therapy? J. Clin. Oncol. *28,* 4769-4777.

Rocha, C.M., Barros, A.S., Gil, A.M., Goodfellow, B.J., Humpfer, E., Spraul, M., Carreira, I.M., Melo, J.B., Bernardo, J., Gomes, A.*, et al.* (2010). Metabolic profiling of human lung cancer tissue by 1H high resolution magic angle spinning (HRMAS) NMR spectroscopy. J Proteome. Res. *9,* 319-332.

Romero-Garcia, S., Lopez-Gonzalez, J.S., Baez-Viveros, J.L., Aguilar-Cazares, D., and Prado-Garcia, H. (2011). Tumor cell metabolism: an integral view. Cancer. Biol. Ther. *12,* 939-948.

Sakai, M., Matsumoto, M., Tujimura, T., Yongheng, C., Noguchi, T., Inagaki, K., Inoue, H., Hosooka, T., Takazawa, K., Kido, Y*., et al.* (2012). CITED2 links hormonal signaling to PGC-1alpha acetylation in the regulation of gluconeogenesis. Nat. Med. *18,* 612-617.

Sanchez-Cespedes, M., Parrella, P., Esteller, M., Nomoto, S., Trink, B., Engles, J.M., Westra, W.H., Herman, J.G., and Sidransky, D. (2002). Inactivation of LKB1/STK11 is a common event in adenocarcinomas of the lung. Cancer Res. *62,* 3659-3662.

Schroeder, T., Yuan, H., Viglianti, B.L., Peltz, C., Asopa, S., Vujaskovic, Z., and Dewhirst, M.W. (2005). Spatial heterogeneity and oxygen dependence of glucose consumption in R3230Ac and fibrosarcomas of the Fischer 344 rat. Cancer Res. *65,* 5163-5171.

Schulze, A., and Harris, A.L. (2012). How cancer metabolism is tuned for proliferation and vulnerable to disruption. Nature *491,* 364-373.

Scott, W.J., Schwabe, J.L., Gupta, N.C., Dewan, N.A., Reeb, S.D., and Sugimoto, J.T. (1994). Positron emission tomography of lung tumors and mediastinal lymph nodes using [18F]fluorodeoxyglucose. Ann. Thorac. Surg. *58,* 698-703.

Semenza, G.L. (2010). Defining the role of hypoxia-inducible factor 1 in cancer biology and therapeutics. Oncogene *29,* 625-634.

Shackelford, D.B., and Shaw, R.J. (2009). The LKB1-AMPK pathway: metabolism and growth control in tumour suppression. Nat. Rev. Cancer *9,* 563-575.

She, P., Shiota, M., Shelton, K.D., Chalkley, R., Postic, C., and Magnuson, M.A. (2000). Phosphoenolpyruvate carboxykinase is necessary for the integration of

hepatic energy metabolism. Mol. Cell. Biol. *20,* 6508-6517.

Singh, M., and Ferrara, N. (2012). Modeling and predicting clinical efficacy for drugs targeting the tumor milieu. Nat. Biotechnol. *30,* 648-657.

Siu, Y.T., and Jin, D.Y. (2007). CREB--a real culprit in oncogenesis. Febs j. *274,* 3224-3232.

Socinski, M.A. (2004). Cytotoxic chemotherapy in advanced non-small cell lung cancer: a review of standard treatment paradigms. Clin. Cancer Res. *10,* 4210s-4214s.

Sonveaux, P., Vegran, F., Schroeder, T., Wergin, M.C., Verrax, J., Rabbani, Z.N., De Saedeleer, C.J., Kennedy, K.M., Diepart, C., Jordan, B.F.*, et al.* (2008). Targeting lactate-fueled respiration selectively kills hypoxic tumor cells in mice. J. Clin. Invest. *118,* 3930-3942.

Stark, R., Pasquel, F., Turcu, A., Pongratz, R.L., Roden, M., Cline, G.W., Shulman, G.I., and Kibbey, R.G. (2009). Phosphoenolpyruvate cycling via mitochondrial phosphoenolpyruvate carboxykinase links anaplerosis and mitochondrial GTP with insulin secretion. J. Biol. Chem. *284,* 26578-26590.

Stryer, L. (1995). Pentose Phosphyte Pathway and Gluconeogenesis. In Biochemistry, Stryer, L. ed., (New York: Freeman WH) pp. 559-580.

Thomlinson, R.H., and Gray, L.H. (1955). The histological structure of some human lung cancers and the possible implications for radiotherapy. Br. J. Cancer *9,* 539-549.

Tsai, W.W., Niessen, S., Goebel, N., Yates, J.R.,3rd, Guccione, E., and Montminy, M. (2013). PRMT5 modulates the metabolic response to fasting signals. Proc. Natl. Acad. Sci. U. S. A. *110,* 8870-8875.

Vander Heiden, M.G., Cantley, L.C., and Thompson, C.B. (2009). Understanding

the Warburg effect: the metabolic requirements of cell proliferation. Science *324,* 1029-1033.

Vaupel, P. (2008). Hypoxia and aggressive tumor phenotype: implications for therapy and prognosis. Oncologist *13 Suppl 3,* 21-26.

Viollet, B., Guigas, B., Leclerc, J., Hebrard, S., Lantier, L., Mounier, R., Andreelli, F., and Foretz, M. (2009). AMP-activated protein kinase in the regulation of hepatic energy metabolism: from physiology to therapeutic perspectives. Acta Physiol. (Oxf) *196,* 81-98.

Vytla, V.S., and Ochs, R.S. (2013). Metformin increases mitochondrial energy formation in L6 muscle cell cultures. J. Biol. Chem. *288,* 20369-20377.

Walenta, S., Snyder, S., Haroon, Z.A., Braun, R.D., Amin, K., Brizel, D., Mueller-Klieser, W., Chance, B., and Dewhirst, M.W. (2001). Tissue gradients of energy metabolites mirror oxygen tension gradients in a rat mammary carcinoma model. Int. J. Radiat. Oncol. Biol. Phys. *51,* 840-848.

Warburg, O., Wind, F., and Negelein, E. (1927). The Metabolism of Tumors in the Body. J. Gen. Physiol. *8,* 519-530.

Watford, M., Hod, Y., Chiao, Y.B., Utter, M.F., and Hanson, R.W. (1981). The unique role of the kidney in gluconeogenesis in the chicken. The significance of a cytosolic form of phosphoenolpyruvate carboxykinase. J. Biol. Chem. *256,* 10023-10027.

Wohlkoenig, C., Leithner, K., Deutsch, A., Hrzenjak, A., Olschewski, A., and Olschewski, H. (2011). Hypoxia-induced cisplatin resistance is reversible and growth rate independent in lung cancer cells. Cancer Lett. *308,* 134-143.

Wu, H., Ding, Z., Hu, D., Sun, F., Dai, C., Xie, J., and Hu, X. (2012). Central role of lactic acidosis in cancer cell resistance to glucose deprivation-induced cell death. J. Pathol. *227,* 189-199.

Xiong, Y., Lei, Q.Y., Zhao, S., and Guan, K.L. (2011). Regulation of glycolysis and gluconeogenesis by acetylation of PKM and PEPCK. Cold Spring Harb. Symp. Quant. Biol. *76,* 285-289.

Yang, J., Kalhan, S.C., and Hanson, R.W. (2009a). What is the metabolic role of phosphoenolpyruvate carboxykinase? J. Biol. Chem. *284,* 27025-27029.

Yang, J., Reshef, L., Cassuto, H., Aleman, G., and Hanson, R.W. (2009b). Aspects of the control of phosphoenolpyruvate carboxykinase gene transcription. J. Biol. Chem. *284,* 27031-27035.

Ye, J., Kumanova, M., Hart, L.S., Sloane, K., Zhang, H., De Panis, D.N., Bobrovnikova-Marjon, E., Diehl, J.A., Ron, D., and Koumenis, C. (2010). The GCN2-ATF4 pathway is critical for tumour cell survival and proliferation in response to nutrient deprivation. Embo J. *29,* 2082-2096.

Yoon, J.C., Puigserver, P., Chen, G., Donovan, J., Wu, Z., Rhee, J., Adelmant, G., Stafford, J., Kahn, C.R., Granner, D.K., Newgard, C.B., and Spiegelman, B.M. (2001). Control of hepatic gluconeogenesis through the transcriptional coactivator PGC-1. Nature *413,* 131-138.

Zhao, S., Xu, W., Jiang, W., Yu, W., Lin, Y., Zhang, T., Yao, J., Zhou, L., Zeng, Y., Li, H.*, et al.* (2010). Regulation of cellular metabolism by protein lysine acetylation. Science *327,* 1000-1004.

10. Appendix

10.1. Protocol PEPCK activity assay

I. Preparation of reagents
Keep NADH in the dark during/after thawing

Preparation of ready-to-use reaction mixtures (On ice)

STOCK	Reaction mixture A (incl CO_2/HCO_3^-)	Reaction mixture B (excl CO_2/HCO_3^-)	Reaction mixture blank	Reaction mixture NADH standard
	[µl]	[µl]	[µl]	[µl]
250mM Imidazole	2933	2933	1760	440
MnCl2	200	200	120	30
NaF	173	173	104	26
Phenylalanine	667	667	400	100
Rotenone	7	7	4	1
PEP	133	133	80	20
NaHCO3	400	0	0	0
NADH	50	50	0	7.5
Malate dehydr	4.5	4.5	2.68	0.6667
H_2O	432	832	530	125
TOTAL	5000	5000	4000	750

II.CO_2 bubbling
*Gas Reaction mixture A 20 min with 100% CO_2 in falcon tube.

III. Cell lysates
Cells are plated at 5.2 Mio/ flask into 75 cm2 flasks. After pretreatment cells are washed 1x with PBS, scraped with PBS, collected, centrifuged, and resuspended in isolation buffer (350 to 500 µl), sonicated 3 x 5 sec on ice. Centrifuged at 7200 rpm (5000 g) for 10 minutes and then supernatant is used for analysis.

Protein concentration is measured in 1:10 diluted samples (BCA). Adjusted to required final concentration of with isolation buffer (to total volume of 250 µl).

IV. Standards
(in duplicates)
Prepare
a) “BLANK”= 2400 µl Reaction mixture blank + 480 µl Isolation buffer + 320 µl H_2O
b) “NADH”= 675 µl Reaction mixture NADH standard + 135 µl Isolation buffer + 90 µl H_2O

*In wells: add 200 µl „BLANK“ to all wells except the wells which have 0.15 mM NADH as final concentration– pipet dilution row with 200 µl „NADH“ solution in duplicates.
Final standard curve NADH concentrations [mM]: 0.15, 0.075, 0.0375, 0.01875, 0.009375, 0.004687, 0.002343.

V. Pipetting of probes

(in triplicates)

*Add **150 µl** reaction mix, with or without HCO_3^-/CO_2 bubbling (no HCO_3^-/CO_2 control=neg control)
*Add homogenate **30 µl** to each well –
*Allow plate to equilibrate to 37°C in heater for 5 minutes
*To initiate reaction add **20µl** of 5 mM dGDP (final concentration 0.5 mM): start with no HCO_3^-/CO_2, then samples with HCO_3^-/CO_2 (1 row), mix with multipipette and immediately read

VI. NADH kinetics measurements

*Measure on Fluo Star at 80 sec intervals. Excitation: 355 nm, emission: 460 nm; 37°C; duration: app. 45 min (35 cycles)
*Calculate slope in linear range of curves.

10.2. Publications by K. Leithner related to the dissertation

Leithner, K., Hrzenjak, A., Trötzmüller, M., Moustafa, T., Köfeler, H.C., Wohlkoenig, C., Stacher, E., Lindenmann, J., Harris, A.L., Olschewski, A., and Olschewski, H. (2014b). PCK2 activation mediates an adaptive response to glucose depletion in lung cancer. Oncogene *2014* Mar 17. doi: 10.1038/onc.2014.47. [Epub ahead of print]

Leithner, K., Wohlkoenig, C., Stacher, E., Lindenmann, J., Hofmann, N.A., Gallé, B., Guelly, C., Quehenberger, F., Stiegler, P., Smolle-Jüttner, F.M., Philipsen, S., Popper, H.H., Hrzenjak, A., Olschewski, A., Olschewski, H. (2014). Hypoxia increases membrane metallo-endopeptidase expression in a novel lung cancer ex vivo model - role of tumor stroma cells. BMC Cancer *14,* 40.